

Molecular phylogenetics of sub-Saharan African natricine snakes, and the biogeographic origins of the Seychelles endemic *Lycognathophis seychellensis*

| | |
|---------------|---|
| Item Type | Journal article |
| Authors | Deepak, V;Maddock, Simon T;Williams, Rhiannon;Nagy, Zoltán T;Conradie, Werner;Rocha, Sara;James Harris, D;Perera, Ana;Gvoždík, Václav;Doherty-Bone, Thomas M;Kamei, Rachunliu G;Menegon, Michele;Labisko, Jim;Morel, Charles;Cooper, Natalie;Day, Julia J;Gower, David J |
| Citation | Deepak, V., Maddock, S.T., Williams, R. et al. (2021) Molecular phylogenetics of sub-Saharan African natricine snakes, and the biogeographic origins of the Seychelles endemic <i>Lycognathophis seychellensis</i> . <i>Molecular Phylogenetics and Evolution</i> , 161, Article Number 107152. https://doi.org/10.1016/j.ympev.2021.107152 |
| DOI | 10.1016/j.ympev.2021.107152 |
| Publisher | Elsevier |
| Journal | <i>Molecular Phylogenetics and Evolution</i> |
| Download date | 2025-05-19 01:17:47 |
| License | https://creativecommons.org/licenses/by-nc-nd/4.0/ |
| Link to Item | http://hdl.handle.net/2436/624015 |

Title: Molecular phylogenetics of sub-Saharan African natricine snakes, and the biogeographic origins of the Seychelles endemic *Lycognathophis seychellensis*

Author names and affiliations:

V. Deepak^{a*}, Simon T. Maddock^{a,b,c,d}, Rhiannon Williams^{a,e}, Zoltán T. Nagy^f, Werner Conradie^{g,h}, Sara Rochaⁱ, D. James Harris^j, Ana Perera^j, Václav Gvoždík^{k,l}, Thomas M. Doherty-Bone^{a,m}, Rachunliu G. Kamei^a, Michele Menegon^{n,o}, Jim Labisko^{c,d,p}, Charles Morel^q, Natalie Cooper^a, Julia J. Day^c & David J. Gower^{a,d}

*Author for correspondence

veerappandeepak@gmail.com

^a *Department of Life Sciences, The Natural History Museum, London SW7 5BD, UK*

^b *School of Biology, Chemistry and Forensic Science, Wolverhampton University
WV1 1LY, UK*

^c *Department of Genetics, Evolution and Environment, University College London,
London WC1E 6BT, UK*

^d *Island Biodiversity and Conservation Centre, University of Seychelles, Mahé,
Seychelles*

^e *NRA Environmental Consultants, Cairns, Queensland 4870, Australia*

^f *Independent Researcher, Berlin, Germany*

^g *Port Elizabeth Museum (Bayworld), Humewood, Port Elizabeth 6013, South Africa*

^h *School of Natural Resource Management, George Campus, Nelson Mandela
University, George 6530, South Africa*

^l *Biomedical Research Center (CINBIO), University of Vigo & Galicia Sur Health Institute, Vigo, Spain*

^j *CIBIO-InBIO, Centro de Investigação em Biodiversidade e Recursos Genéticos, University of Porto, 4485-661 Vairão, Portugal*

^k *Institute of Vertebrate Biology of the Czech Academy of Sciences, Brno, Czech Republic*

^l *National Museum, Department of Zoology, Prague, Czech Republic*

^m *Conservation Programs, Royal Zoological Society of Scotland, Edinburgh EH12 6TL, UK*

ⁿ *Division of Biology & Conservation Ecology, Manchester Metropolitan University, UK*

^o *PAMS Foundation, P.O. Box 16556, Arusha, Tanzania*

^p *Durrell Institute of Conservation and Ecology, School of Anthropology and Conservation, University of Kent, Canterbury CT2 7NR, UK*

^q *Natural History Museum, Victoria, Mahé, Seychelles*

Declaration of interest: None

Acknowledgements:

VD was funded by EU Marie Skłodowska-Curie Fellowship 751567. STM was funded by an NHM-UCL IMPACT PhD studentship. STM and JL each received awards from the Systematics Research Fund of the Systematics Association and Linnean Society of London, and the Mohammed bin Zayed Conservation Fund (Projects 172515128 and 162513749). Seychelles research was also funded by the BBSRC's SynTax scheme (awarded to M. Wilkinson, JJD and DJG). VG was supported by the IVB CAS institutional support (RVO: 68081766), and the Ministry of Culture of the Czech Republic (DKRVO 2019–2023/6.VII.c, National Museum, 00023272). TDB's fieldwork was funded by the Royal Geographical Society, and Golder Associates. RGK received EU Marie Skłodowska-Curie Fellowship (PIIF-GA-2013-625870). This work was also supported by Darwin Initiative grant 19-002 (to J.J. Groombridge and colleagues). For the Seychelles component we thank Aaron Bauer, Berthilde Belle, Rachel Bristol, Lyndsay Chong-Seng, Beryl Ondiek, Jeff Streicher and Mark Wilkinson for help with logistics and sampling, and companionship in the field, the Seychelles Bureau of Standards for providing required field collection permits, and our Seychelles Darwin Initiative grant project partners: Seychelles National Park Authority, Seychelles Islands Foundation, Island Conservation Society, National Museum of Seychelles, and the Ministry of Environment. For help with the Praslin fieldwork, we especially thank Nancy Bunbury, Wilna Accouche, Marc Jean-Baptiste and other staff at the Vallée de Mai. We thank the late Bill Branch for contributing some African samples. WC thanks Brian Huntley for organising the Lagoa Carumbo Expedition in 2011 (National Geographic Society grant number 891-11), Chris Brooks for organising the Southern Africa Regional Environmental Program's (SAREP) Aquatic Biodiversity Survey of the lower Cuito and Cuando Rivers in Angola in 2013, the National Geographic Okavango Wilderness Project (National Geographic Society

grant number EC0715–15) for funding fieldwork to Angola 2015–2019, and the Angolan Ministry of Environment (MINAMB) for issuing permits. VD thanks Gabriela Bittencourt-Silva, Ana Serra Silva and Gontran Sonet for practical assistance, GBIF for open access distribution data, and Maria Chiara Deflorian (Museo delle Scienze, Trento, Italy) for loaning specimens of *Natriciteres* to London. We thank the following Alan Resetar (Field Museum (FMNH), Chicago) and Lauren Scheinberg (California Academy of Sciences (CAS), California) for making tissue samples available for this study. VD thanks Jeff Streicher and Ana Serra Silva for their help with the TreePL analysis and discussions on molecular dating analysis.

Abstract:

Phylogenetic relationships of sub-Saharan African natricine snakes are understudied and poorly understood, which in turn has precluded analyses of the historical biogeography of the Seychelles endemic *Lycognathophis seychellensis*. We inferred the phylogenetic relationships of Seychelles and mainland sub-Saharan natricines by analysing a multilocus DNA sequence dataset for three mitochondrial (mt) and four nuclear (nu) genes. The mainland sub-Saharan natricines and *L. seychellensis* comprise a well-supported clade. Two maximally supported sets of relationships within this clade are (*Limnophis*, *Natriciteres*) and (*Afronatrix*, (*Hydraethiops*, *Helophis*)). The relationships of *L. seychellensis* with respect to these two lineages are not clearly resolved by analysing concatenated mt and nu data. Analysed separately, nu data best support a sister relationship of *L. seychellensis* with (*Afronatrix*, (*Hydraethiops*, *Helophis*)) and mt data best support a sister relationship with all mainland sub-Saharan natricines. Methods designed to cope with incomplete lineage sorting strongly favour the former hypothesis. Genetic variation among up to 33 *L. seychellensis* from five Seychelles islands is low. Fossil calibrated divergence time estimates support an overseas dispersal of the *L. seychellensis* lineage to the Seychelles from mainland Africa ca. 43–25 Ma, rather than this taxon being a Gondwanan relic.

Key Words: biogeography, Gondwana, Natricinae, Natricidae, overseas dispersal, systematics

1. Introduction

The Seychelles archipelago is an unusual island system in that it has both a remote, oceanic setting and continental origins as a fragment of Gondwana. Thus, its extant biota is a mosaic of ancient, relictual lineages and more recent overwater arrivals (Ali, 2017). This provides an attractive system for studying evolutionary processes, though exploiting this system for evolutionary research depends on improved knowledge of whether each resident lineage is ancient or relatively recent, as well as the status of populations on multiple Seychelles islands. Recently, some of this information has been generated for several lineages of Seychelles amphibians and reptiles (e.g., Brandley et al., 2005; Rocha et al., 2010, 2011, 2016a, b; Tolley et al., 2013; Maddock et al., 2014), but not yet for any of the native snakes (see Williams et al., 2020 for the latest assessment of the non-native status of Seychelles *Indotyphlops braminus*).

The snake *Lycognathophis seychellensis* (Schlegel, 1837) is endemic to the granitic islands of the Seychelles (Nussbaum, 1984). Several aspects of the systematics and historical biogeography of *L. seychellensis* remain unclear. DNA sequence data (for two partial nuclear genes, *cmos* and *rag2*) have been published for only one or two individuals of *L. seychellensis* (Vidal et al., 2008). This species has been recorded from six of the inner, granitic Seychelles islands (Fig. 1; Gerlach and Ineich, 2006) and exhibits notable colour polymorphism (Nussbaum, 1984). Other Seychelles reptile species have been found to display high levels of variation within and among islands, with potential implications for taxonomy and conservation management (Rocha et al., 2011, 2013, 2016; Valente et al., 2014; Harris et al., 2015). Thus, an inspection of possibly substantial intraspecific genetic variation in *L. seychellensis* is warranted.

Currently there are 252 recognised species in the colubrid subfamily Natricinae, with the majority of this diversity found in Asia (183 species ca. 72%), only 13 species (ca. 5%) in mainland sub-Saharan Africa, and none in Madagascar (Uetz et al, 2020). Previous molecular phylogenetic analyses (Vidal et al., 2008; Dubey et al., 2012; Guo et al., 2012; Pyron et al., 2013; Zaher et al., 2019) supported the natricine colubrid (natricid according to some classifications: e.g., Zaher et al., 2019) identity of *L. seychellensis* proposed by Dowling (1990) based on vertebral and hemipenial anatomy, and indicated a close relationship with (and possible membership of) a mainland sub-Saharan African natricine radiation. However, those studies sampled only three of the six extant sub-Saharan African natricine genera (see Fig. 1 for distribution map) and only four of the 13 currently recognised species. Additionally, those previous studies disagreed as to whether *L. seychellensis* is more closely related to *Afronatrix* (Dubey et al., 2012; Pyron et al., 2013; Zaher et al., 2019) or to *Natriciteres* (Guo et al., 2012). As far as we are aware, there are no phylogenetic hypotheses that include all mainland sub-Saharan African natricine genera such that, beyond the close inferred relationship of the only two previously sampled genera in molecular phylogenetic studies (*Afronatrix* and *Natriciteres*), there appears to have been no previous consideration as to whether the mainland sub-Saharan African natricines constitute a single radiation and what their biogeographic origins might be. Finally, there are no published estimates of the age of the split between *L. seychellensis* and its closest extant relative. Having this temporal framework would allow a test of the hypothesis that the *L. seychellensis* lineage arrived in the Seychelles via overseas dispersal rather than being a Gondwanan relic.

Here we present analyses of mitochondrial and nuclear DNA sequence data in order to test the following hypotheses: (1) mainland sub-Saharan African natricines are monophyletic, (2) *L. seychellensis* lies within the sub-Saharan African radiation, (3) intraspecific genetic variation within *L. seychellensis* is low across multiple Seychelles islands, and (4) the *L. seychellensis* lineage arrived in the Seychelles via oceanic dispersal rather than being an ancient, Gondwanan relic.

2. Materials and Methods

2.1. DNA sequence data generation and alignment

To infer phylogenetic relationships and to assess intraspecific genetic variation within the Seychelles endemic *Lycognathophis seychellensis*, we generated mitochondrial (mt) and nuclear (nu) gene sequence data for a total of 33 specimens of this species from across five of the six islands of its known distribution (Table 1). This included 14 individuals from Mahé, six from Praslin, six from Silhouette, two from La Digue, and five from Frégate. The eight partial genes sequenced were mt *16s* (n = 30), *cytb* (n = 29) and *nd4* (n = 2), and nu *cmos* (n = 8), *nt3* (n = 8), *bdnf* (n = 6), *rag1* (n = 2), and *prlr* (n = 21). In addition to the new *L. seychellensis* data, we generated 119 sequences for the three mt genes (*16s*, *cytb*, *nd4*) and four of the nuDNA loci (*cmos*, *nt3*, *bdnf*, *rag1*) for 27 other natricine snakes representing ten mainland sub-Saharan African species and five Asian species (Table 1).

Genomic DNA was extracted from muscle, liver, tail tip or ventral scale clip tissue samples stored in absolute ethanol at -20°C, using the DNeasy (Qiagen™) blood and tissue kit. Primers and annealing temperatures for PCR amplification and for sequencing are reported in Table S1. Bidirectional sequence chromatograms were edited and assembled using Chromas Lite v. 2.1.1 (Technelysium, 2012).

Possibly heterozygous positions in nuDNA sequences were given ambiguity codes. MEGA v. 7.0 (Kumar et al., 2016) was used to assemble sequences. Protein-coding sequences were checked for unexpected stop codons by translating nucleotide alignments to amino acids. Newly generated data were combined with data from GenBank for other natricines and outgroups (Table 1), and aligned using the ClustalW algorithm (Thompson et al., 1994) with default settings as implemented in MEGA.

2.2. Molecular phylogenetics

To infer the phylogenetic relationships of *L. seychellensis* and mainland sub-Saharan African natricines, we assembled a dataset of sequences from GenBank (Benson et al., 2017) and our newly generated sequences for three mitochondrial (*16s*, *cytb*, *nd4*) and four nuclear (*cmos*, *nt3*, *bdnf*, *rag1*) genes. Initially we ran analyses with a 157-leaf dataset, comprising 155 natricines and two colubroid outgroups; the grayiine (grayiid) *Grayia ornata* and sibynophiine (sibynophiid) *Sibynophis subpunctatus* (Table S2). Outgroup selection was based on the results of more broadly sampled molecular phylogenetic studies (Figuroa et al. 2016; Zaher et al. 2019; Lalronunga et al. 2020). The 155 natricines comprised 26 sub-Saharan African (including Seychelles) leaves representing all six genera and eleven of the 14 currently recognised species. The other 129 natricine leaves were selected from across the global geographic and phylogenetic diversity of the group based on each leaf being represented by at least three of the seven genes included in the dataset. This sampling covered 30 of the 36 genera and 115 of the 245 species of extant natricines currently recognised (Uetz et al., 2020). Based on results of maximum likelihood (ML) (Felsenstein, 1981) analyses of concatenated data for this 157-leaf

dataset, in which sub-Saharan and Seychelles natricines were together maximally supported as monophyletic, we subsequently ran phylogenetic analyses for a more restricted 21-leaf dataset (Table 1, Table S2) in an attempt to run phylogenetic analyses using (hopefully, more realistic) models estimated for a more focused taxon set with more complete data. This comprised 17 Seychelles and mainland sub-Saharan African natricines plus four outgroup natricines selected from among the likely closest relatives of the Seychelles + mainland sub-Saharan African clade. This dataset is also a combination of GenBank and newly generated sequences (Table S2).

Phylogenetic analyses were carried out using the CIPRES Science Gateway v3.3 (Miller et al., 2010). We applied ML using RAxML-HPC2 on XSEDE v. 8.2.12 (Stamatakis, 2014), and Bayesian inference (BI) analysis using MrBayes v. 3.2.6 on XSEDE (Ronquist et al., 2012). PartitionFinder2 (Lanfear et al., 2016) was used to determine best-fit gene and codon partitioning strategies using the greedy algorithm and BIC model selection, departing from gene and codon position blocks. RAxML analyses applied the GTRGAMMA model (following Stamatakis, 2006) to each partition. For the BI analysis we executed two runs with four Markov chains initiated from random trees and ran these for 10,000,000 generations each, sampling every 1000 generations. When the BI analysis was terminated, the standard deviation of split frequencies was less than 0.005, and the first 25% trees were discarded as “burn-in”. Convergence was assessed for all parameters using Tracer v1.6 (Rambaut et al., 2014) and the RWTY package (Warren et al., 2017). BI analysis used best-fit models as determined by PartitionFinder. Support for internal branches was quantified using bootstrap proportions (calculated from 500 replicates) and Bayesian posterior probabilities, respectively.

We compared the fit of the data to optimal and best suboptimal trees for both ML and BI analyses for the 21-leaf dataset. For ML, we assessed differences in likelihood between optimal and suboptimal trees using the Approximately Unbiased (AU; Shimodaira, 2002) and Shimodaira-Hasegawa (SH; Shimodaira and Hasegawa, 1999) tests as implemented in the package CONSEL (Shimodaira and Hasegawa, 2001). For BI, we used Bayes factors (Kass and Raftery, 1995), with Marginal Likelihood estimate (MLE) scores estimated using path sampling and steppingstone sampling methods as described by Baele et al. (2012, 2013). Using BEAST v 1.10.4, analyses applying each of the alternative tree topologies as constraints were each run for 150,000,000 generations and sampled every 5,000. MLE scores were generated from 100 path steps for each run for 500,000 generations.

A species tree analysis of the 21-leaf dataset was carried out using a Bayesian multispecies coalescent approach as implemented in StarBEAST2 (BEAST v2.5, Bouckaert et al., 2019). Input files for StarBEAST2 were prepared using BEAUti 2 (Drummond et al., 2012). Each terminal was assigned to a described species. Priors were set as follows: linked tree model, strict clock, constant root population size model on species tree, GTR model for each locus, analyses initiated with a random starting tree for each locus, population mean set to a uniform prior and a lognormal prior for population size. The analysis was run for 100,000,000 generations sampling every 10,000 generations following a 10% burn-in. Convergence was checked in Tracer V1.6 with ESS \geq 200. Resulting trees were summarised in LogCombiner 2.4.4 and TreeAnnotator 2.5. (Bouckaert et al., 2019). Results were visualised in FigTree 1.4.3 (Rambaut, 2016) and DensiTree (Bouckaert and Heled, 2014).

We compared support for alternative resolutions of the relationships of *L. seychellensis* under ML and BI analyses of the 21-leaf, concatenated mt and nu dataset. Support values were read from majority rule partition tables in PAUP* (Swofford, 2000) for 500 RAxML bootstrap trees, 2,000 sampled (post burn-in) MrBayes BI trees, and 1,500 sampled (post burn-in) BEAST2 BI trees. For RAxML, analyses were carried out with data partitioned by gene and by gene and codon position.

2.3. Divergence time estimation & historical biogeography

Our main aim was to test the hypothesis that the Seychelles natricine lineage reached the Seychelles via overseas dispersal, rather than being a Gondwanan relic. The geological timeframe for this test is as follows. Following the initial break up of eastern and western Gondwana from ca. 165 million years before present (Ma), Indo-Madagascar split from Antarctica+Australia ca. 130–112 Ma, and Madagascar split from India+Seychelles from ca. 88 Ma (see Samonds et al., 2012). Finally, India and Seychelles separated ca. 71–63 Ma (Collier et al., 2008; Minshull et al., 2008; Armitage et al., 2011; Ganerød et al., 2011; see Gower et al., 2016).

To estimate the age of the divergence between *L. seychellensis* and its closest extant relative, we analysed a taxonomically reduced dataset of 73 leaves to decrease computational time required for analyses (Table 2). This includes 12 natricines, including one *L. seychellensis*, and nine mainland sub-Saharan African natricines (eight currently recognised species). In addition, we included 61 non-natricines in the dataset in order to make use of some of the best fossil calibrations available for snakes (see Head 2015, 2016; Zaher et al., 2019). Beyond the seven genes for which we generated new data, we also included an additional region in

rag1 (Wiens et al., 2008) because sequences of this marker were available for almost 40% of the samples. This dataset included in total 5,021 base pairs (Table 2). The data were newly aligned and the best-fit gene and codon partitioning scheme (Table S3) was selected using PartitonFinder2 as reported above.

We applied seven fossil calibrations, largely those recommended by Head (2015) and Head et al. (2016): (1) oldest divergence within crown Alethinophidia based on *Hassiophis terrasanctus* (Tchernov et al., 2000); minimum age 93.9; (2) divergence between non-xenodermid colubrids and their closest living relative (Xenodermidae in our tree) based on *Procerophis sahnii* (Rage et al., 2008); minimum age 50.5 Ma; (3) divergence between Boinae and its sister taxon (Erycinae + Candoiinae in our tree) based on *Titanoboa cerrejonensis* (Head et al., 2009); minimum age 58 Ma; (4) divergence between *Corallus* and (*Chilabothrus*, (*Epicrates*, *Eunectes*)); *Corallus priscus* (Rage, 2001); minimum 50.2 Ma; (5) divergence between Viperinae and Crotalinae based on *Vipera aspis* complex (Szyndlar and Rage, 1999); minimum age 20.0 Ma; (6) divergence between *Acrochordus javanicus* and (*A. arafurae*, *A. granulatus*) based on *Acrochordus dehmi* (Hoffstetter, 1964); minimum age 18.1 Ma and (7) oldest divergence between *Naja* (*Afronaja*) and *Naja* (*Boulengerina*) based on *Naja romani* (Hoffstetter, 1939) (A.B. Quadros pers. comm. 2019, based on work presented by Quadros et al., 2019); minimum age 17 Ma. Input values applied to each calibration prior are reported in Table S4.

Dating analyses were carried out using the CIPRES Science Gateway v3.3 (Miller et al., 2010). We estimated divergence times using BEAST2 on XSEDE v2.6 (Bouckaert et al., 2019) under a Yule tree prior. A relaxed lognormal clock was assigned for each partition of the concatenated BEAST2 analysis. We set up two

independent runs, the Markov Chain Monte Carlo (MCMC) was run for 200,000,000 generations sampling every 10,000 trees, and effective sample size (ESS) values were evaluated using Tracer v. 1.7 (Rambaut et al., 2014). Initial runs applied the best-fit partitioning scheme and models, but this resulted in poor mixing of the GTR model parameters for partitions 1, 2, 3 & 4. We therefore repeated BEAST2 analyses implementing the less complex HKY model for these partitions. Additionally, we estimated divergence dates using Penalized Likelihood (Sanderson, 2002) as implemented in TreePL (Smith and O'Meara, 2012), applying the fossil dates above for calibrations 1–7 as hard minimum and maximum ages. Penalized likelihood uses a tree with branch lengths and calibrations without prior parametric distributions. We ran TreePL with 10,000 iterations and a smoothing parameter of 100.

Historical biogeography was investigated by estimating ancestral areas for the dated phylogeny using dispersal-extinction-cladogenesis (DEC; Ree et al., 2005, 2008) and dispersal-vicariance analysis (DIVALIKE; Ronquist, 1997; Ronquist and Sanmartín, 2011) models implemented in BioGeoBEARS v.1.1 (Matzke, 2013) in R v 4.0 (R Core Development Team, 2020). We also implemented these models using the peripatric speciation "*j*" ('jump') parameter, which although criticised by Ree and Sanmartín (2018), is often the most biologically realistic scenario for colonization and subsequent divergence on remote islands (Tsang et al., 2020). We defined three areas: Asia, Seychelles, and mainland sub-Saharan Africa, and set the maximum number of ancestral areas to three, because this was the maximum number of areas occupied by any clade in our analysis. We compared the fit of these four models (DEC, DEC + *j*, DIVALIKE and DIVALIKE + *j*) using Akaike Information Criterion (AIC) scores and weights.

2.4. Genetic diversity within *Lycognathophis seychellensis*

PopArt (Leigh and Bryant, 2015) was used to generate haplotype networks to display intraspecific variation for *L. seychellensis* for *16s* and *cytb* under the median-joining algorithm (Bandelt et al., 1999).

3. Results

3.1. Molecular phylogenetics

The best-fit partitioning scheme for the 21-leaf dataset comprised six partitions, by gene and by codon position (Table S5). Mainland sub-Saharan African natricines plus *L. seychellensis* are strongly supported as monophyletic (Fig. 2A), and almost all intergeneric relationships within this lineage are well supported. In particular, and denoting the mainland sub-Saharan African genera with the first two letters of their name, the two sets of relationships (*Li,Na*) and (*Af,(He,Hy)*) are maximally supported (Fig. 2B). The relationship of *L. seychellensis* to these two lineages is less clearly resolved in analyses of the concatenated nu and mt data. In the 157-leaf dataset, *L. seychellensis* is sister to (*Af,(He,Hy)*), with ML bootstrap and Bayesian posterior probability support of 63 and 0.97, respectively (Fig. S1). The same relationship was recovered in ML(RAxML) analysis of the 21-leaf dataset, with lower support (37%), but in the BI (MrBayes) analysis of this dataset, *L. seychellensis* is instead sister to all mainland sub-Saharan African natricines (support for monophyly of the latter clade 0.59) (Fig. 2; Table 3).

Examination of majority rule partition tables in PAUP* (Swofford, 2000) for the 500 RAxML ML bootstrap trees and 2,000 post-burnin MrBayes BI trees for the 21-leaf dataset shows that support is lowest for the third alternative resolution of the position of *L. seychellensis* with respect to (*Li,Na*) and to (*Af,(He,Hy)*), that is, as

sister to the former clade (*Li,Na*), which receives support of only 27% (RAxML) and 0.12 (MrBayes) (Table 3). For the ML analysis, these support values are very similar when the same dataset is partitioned by gene instead of by gene and codon (Table 3). Both the AU and SH tests indicate that differences in likelihood between the fit of the three alternative topologies to the data are not significant (Table 4). Bayes factors indicate that the differences in fit to the data among the three alternative topologies are also not substantial, but differences in fit to data between the trees with *L. seychellensis* as sister to (*Af,(He,Hy)*) and as sister to either (*Li,Na*) or to ((*Li,Na*)(*Af,(He,Hy)*)) are greater than differences in fit to data between the trees with the latter two sets of relationships (Table 4).

Analysis of the 21-leaf dataset for the nu and the mt data separately reveals that incongruence between these partitions explains a substantial part of the lack of compelling resolution of the relationships of *L. seychellensis* in analyses of the concatenated data. For the mt data, *L. seychellensis* is most strongly supported as sister to (*Af,(He,Hy)*), whereas for the nu data this is the least well supported of the three alternative resolutions, with instead *L. seychellensis* as sister to (*Af,(He,Hy)*) receiving the most support (Table S6). The Bayesian multispecies coalescent analysis using StarBEAST yielded 17,998 trees with 43 different topologies. Among these trees, 98% included *L. seychellensis* as sister to (*Af,(He,Hy)*).

3.2. Divergence dating & historical biogeography

When applying the HKY model in BEAST2 analyses, to those partitions for which good mixing was not achieved when applying GTR, good mixing was achieved for all parameters, for posteriors and priors (ESS > 200). Highest posterior density (HPD) intervals are wide for divergence times estimated in BEAST2 analyses. In

unconstrained BEAST2 analysis, *L. seychellensis* is recovered as sister to the mainland sub-Saharan African (*Af*,(*He*,*Hy*)), with the split between these two lineages estimated to have occurred with a 95% HPD interval of 43.2–24.6 Ma (mean 35.3 Ma) (Fig. 3; Fig.S2), which is similar to the TreePL estimate of this divergence time for this node, at 35.7 Ma.

Enforcing the two alternative competing resolutions (from separate mt and nu data analyses) of the relationships among *L. seychellensis* and (*Af*,(*He*,*Hy*)) and (*Li*,*Na*) yields similar time estimates for the split between *L. seychellensis* and its closest extant (mainland sub-Saharan African) relative (Table 5). For BEAST2 runs applying GTR, as suggested by PartitionFinder2 results, ESS values were low for posterior (46) and prior (37) distributions, though the divergence date in question was similarly estimated (Fig. S3).

All of the BioGeoBEARS analyses agree with each other and with parsimony (carried out manually; results not shown) in their estimation of all ancestral areas. Asia is the estimated ancestral area for the sampled taxa, with a dispersal/vicariance event to sub-Saharan Africa. Dispersal rather than vicariance is the most likely explanation for origin of the sub-Saharan African clade because the phylogenetic split with Asian natricines is estimated to be much younger (48.7 Ma; HPD: 34.1–56.6) than the Gondwanan breakup. However, the route of dispersal to sub-Saharan Africa and whether this was via land or sea is open to further investigation. A single dispersal event from mainland Africa to the Seychelles occurred relatively early on in the history of the group (Fig. 3). The divergence between the Seychelles natricine and its closest mainland African relative (35.7 Ma; HPD: 43.2–24.6 Ma) is much younger than the break-up between Seychelles and other Gondwanan landmasses (63 Ma or older, see section 2.3), strongly supporting overseas dispersal. Among the

four models implemented, DEC + *j* was the best fitting, closely followed by DIVALIKE + *j* and DEC (Table 6).

3.3. Intraspecific genetic diversity

Intraspecific genetic diversity across the range of *Lycognathophis seychellensis* is low. Except for five single-site ambiguities (possible heterozygosity) in *prlr* and one in *rag1* there was no variation for any of the five nuclear gene sequences generated. For *16s* and *cytb* there are only two and four segregating sites, and zero and one parsimony informative sites, respectively. Therefore, we generated haplotype networks but not phylogenetic trees to examine spatial patterns in genetic variation (Fig. 4). There is only one instance of a single island having a haplotype not found on other islands, though this single *cytb* haplotype from Silhouette differs from those found on other islands by only a single step.

4. Discussion

4.1. Molecular phylogenetics and genetic diversity

Our molecular phylogenetic analyses are the first to comprehensively sample extant sub-Saharan African (including Seychelles) natricine genera (all six genera, and 11 out of 14 species), and we find compelling support for their monophyly. Our results are consistent with previous work based on morphology that proposed that *Helophis* is a natricine and is closely related to *Hydraethiops* (de Witte, 1922; Broadley, 1998; Nagy et al., 2014), and that *Limnophis* and *Natriciteres* are closely related (Dowling and Duellman, 1978; Zaher, 1999). We were unable to identify with precision and reasonable support the closest living relatives of the sub-Saharan African (including Seychelles) natricine radiation. However, our results point to this

radiation arising from within one of the Asian radiations (the clade excluding New World natricines plus (Eur)Asian *Natrix*, *Sinonatrix*, *Smithophis*, and *Opisthotropis*).

The phylogenetic results regarding the identity of the sister group of *L. seychellensis* are not compelling from the analyses of the concatenated nu and mt sequence data. However, partitioned analyses provide evidence of substantial nu-mt incongruence, and analysis using a multispecies coalescent approach that is designed to cope with incomplete lineage sorting strongly supports the hypothesis that *L. seychellensis* is sister to *Hydraethiops* + *Helophis* + *Afronatrix*.

The almost complete lack of molecular genetic variation within *L. seychellensis* across five Seychelles islands is consistent with there being only a single extant species of natricine occurring on the Seychelles. The very low intraspecific variation contrasts with that found for other native Seychelles squamate reptiles and other taxa (e.g., frogs: Labisko et al., 2019; caecilians: Maddock et al., 2020; crabs: Daniels, 2011), which have substantial and strongly spatially structured, intraspecific molecular genetic variation. This structured variation often includes a distinct genetic lineage on Silhouette, a hint of which is also found here for *L. seychellensis cytb*.

The lack of genetic variation suggests that the current genetic diversity within *L. seychellensis* is the product of a strong founder effect for a relatively recent overseas arrival (not supported by our dating results) and/or within-Seychelles dispersal from a substantially contracted refugial population representing some form of secondary founder effect. Due to the relatively deep phylogenetic divergence of *L. seychellensis* and no record of this taxon occurring beyond Seychelles, a very recent, human mediated dispersal to Seychelles is highly unlikely and can be discounted with confidence. The lack of genetic variation among populations of *L.*

seychellensis from different islands is consistent with this species being a relatively good disperser among the major granitic islands of the Seychelles (perhaps the best of Seychelles squamates studied thus far), across relatively shallow, narrow seas and/or during multiple low sea level stands during the Pleistocene, when these islands would have been repeatedly dis- and reconnected (Warren et al. 2010). A closer examination of *L. seychellensis* intraspecific genetic variation within and among islands using rapidly evolving nuclear markers and a denser sampling would be worthwhile.

4.2. Historical biogeography

Our results are consistent with the *L. seychellensis* lineage reaching the Seychelles via overseas dispersal from Africa, approximately 43–25 Ma. Probably this is a similar mode and timing of origin to all of the other Seychelles native squamate reptiles for which data are available. For example, the endemic Seychelles chameleon *Archaius tigris* is most closely related to East African *Rieppeleon* spp., with the two diverging an estimated 43–27 Ma (Tolley et al., 2013: table S4). The Seychelles skinks *Trachylepis seychellensis* and *T. wrightii* are estimated to have diverged from their closest extant relatives, mostly occurring in Africa, approximately 41–24 Ma (Lima et al., 2013; Weinell et al., 2019). Dating estimates are not yet available for other Seychelles squamates, but native and endemic Seychelles species of geckos of the genera *Phelsuma*, *Urocotyledon* and *Ailuronyx* have closest extant relatives in Africa and/or Madagascar (Rocha et al., 2010; Gamble et al., 2012). The monotypic Seychelles fossorial skinks *Janetaescincus* spp. and *Pamelaescincus gardineri* are sister to a large clade of extant African, Arabian and Indian Ocean island taxa (Brandley et al., 2005).

The origins of Seychelles squamates contrast with those for most of the native amphibians. Although the hyperoliid frog *Tachycnemis seychellensis* arrived from overseas dispersal from Madagascar approximately 35.3–9.8 Ma (Crottini et al., 2012; Maddock et al. 2014; ca. 20–12 Ma based on Portik et al. [2019: fig. S2]), the two ancient Seychelles amphibian lineages that comprise eight indotyphlid caecilian species (Maddock et al., 2017, 2018) and at least four sooglossid frog species have their closest extant relatives in India, and are Gondwanan relics (Wilkinson et al., 2002; Biju and Bossuyt, 2003; Gower et al., 2011, 2016; Kamei et al., 2012; Janani et al., 2017; Labisko et al., 2019).

Globally, natricines are ecologically diverse, utilising ground, shrub and tree, soil, semiaquatic and/or aquatic habitats. Mainland sub-Saharan African natricines, as well as being relatively species poor, are seemingly ecologically more conservative despite being the product of approximately 30 million years of evolution, with perhaps all species being predominantly semiaquatic or even aquatic (Gibbons and Dorcas, 2004; Vitt and Caldwell, 2009). Additional and more detailed ecological data would be useful, but *L. seychellensis* appears to be the only member of the sub-Saharan African (including Seychelles) radiation that is predominantly terrestrial. It is typically encountered on the ground, though can be observed in vegetation at heights of at least 5 m as well as on the margins of pools and streams (STM, JL, RK & DJG pers. obs.). It is not clear whether this disparate ecology is ancestral to the *L. seychellensis* lineage and a factor that might have promoted its overseas dispersal to Seychelles, or whether it is a derived feature acquired since the lineage reached Seychelles. All mainland sub-Saharan African natricines are oviparous. *Lycognathophis seychellensis* is probably also oviparous (Nussbaum, 1984) but direct observations have yet to be reported (Gerlach and Ineich, 2006).

Extant mainland sub-Saharan African natricines are relatively species-poor, comprising only ca. 5% of global natricine diversity. Natricines are unknown from Madagascar or Indian Ocean islands other than Seychelles. As argued for other Indian Ocean and Madagascar taxa, the overseas dispersal of the *L. seychellensis* lineage from mainland Africa eastwards was perhaps assisted by sporadic but strong eastward oceanic currents and large, continental freshwater outflows during the Paleogene (65.5–23 Ma: Ali and Huber, 2010; Townsend et al., 2010).

References

- Armitage, J.J., Collier, J.S., Minshull, T.A., Henstock, T.J., 2011. Thin oceanic crust and flood basalts: India-Seychelles breakup. *Geochem. Geophys. Geosyst.*, 12(5), Q0AB07, <https://doi.org/10.1029/2010GC003316>
- Ali, J.R., Huber, M., 2010. Mammalian biodiversity on Madagascar controlled by ocean currents. *Nature* 463, 653–680. <https://doi.org/10.1038/nature08706>.
- Ali, J.R., 2017. Islands as biological substrates: classification of the biological assemblage components and the physical island types. *J. Biogeogr.* 44(5), 984–994. <https://doi.org/10.1111/jbi.12872>
- Bandelt, H.J., Forster, P., Röhl, A., 1999. Median-joining networks for inferring intraspecific phylogenies. *Mol. Biol. Evol.* 16(1), 37–48. <https://doi.org/10.1093/oxfordjournals.molbev.a026036>
- Baele, G., Lemey, P., Bedford, T., Rambaut, A., Suchard, M.A., Alekseyenko, A.V., 2012. Improving the accuracy of demographic and molecular clock model comparison while accommodating phylogenetic uncertainty. *Mol. Biol. Evol.* 29, 2157–2167. <https://doi.org/10.1093/molbev/mss084>

- Baele, G., Li, W.L.S., Drummond, A.J., Suchard, M.A., Lemey, P., 2013. Accurate modelselection of relaxed molecular clocks in Bayesian phylogenetics. *Mol. Biol. Evol.* 30, 239–243. <https://doi.org/10.1093/molbev/mss243>
- Benson, D.A., Cavanaugh, M., Clark, K., Karsch-Mizrachi, I., Lipman, D.J., Ostell, J., Sayers, E.W., 2017. GenBank. *Nucleic Acids Research*, 45 (Database issue), D37–D42. <https://doi.org/10.1093/nar/gkw1070>
- Biju, S.D., Bossuyt, F., 2003. New frog family from India reveals an ancient biogeographical link with the Seychelles. *Nature* 425(6959), 711. <https://doi.org/10.1038/nature02019>
- Brandley, M.C., Schmitz, A., Reeder, T.W., 2005. Partitioned Bayesian analyses, partition choice, and the phylogenetic relationships of scincid lizards. *Syst. Biol.* 54(3), 373–390. <https://doi.org/10.1080/10635150590946808>
- Broadley, D.G., 1998. The reptilian fauna of the Democratic Republic of the Congo (Congo-Kinshasa). In: Schmidt, K.P., Noble, G.K. (Eds.), *Contributions to the Herpetology of the Belgian Congo*. [reprint of the 1919 and 1923 papers]. SSAR Facsimile reprints in *Herpetology* 780 pp.
- Bouckaert, R., Heled, J., 2014. DensiTree 2: Seeing trees through the forest. *BioRxiv*, 012401.
- Bouckaert R., Vaughan T.G., Barido-Sottani J., Duchêne S., Fourment M., Gavryushkina A., Heled, J., Jones, G., Kühnert, D., De Maio, N., Matschiner, M., 2019. BEAST 2.5: An advanced software platform for Bayesian evolutionary analysis. *PLoS Comput. Biol.* 15(4), e1006650. <https://doi.org/10.1371/journal.pcbi.1006650>
- Chippaux, J.P., Jackson, K., 2019. *Snakes of Central and Western Africa*. John Hopkins University Press, Baltimore, USA.

- Collier, J.S., Sansom, V., Ishizuka, O., Taylor, R.N., Minshull, T.A., Whitmarsh, R.B., 2008. Age of Seychelles-India break-up. *Earth Planet. Sci. Lett.*, 272, 264–277. <https://doi.org/10.1016/j.epsl.2008.04.045>
- Conradie, W., Deepak, V., Keates, C., Gower, D.J., 2020. Kissing cousins: a review of the African genus *Limnophis* Günther, 1865 (Colubridae: Natricinae), with the description of a new species from north-eastern Angola. *Afr. J. Herpetol.*, 69(1), 79–107. <https://doi.org/10.1080/21564574.2020.1782483>
- Crottini, A., Madsen, O., Poux, C., Strauß, A., Vieites, D.R., Vences, M., 2012. Vertebrate time-tree elucidates the biogeographic pattern of a major biotic change around the K–T boundary in Madagascar. *Proc. Natl. Acad. Sci. USA* 109 (14), 5358–5363. <https://doi.org/10.1073/pnas.1112487109>
- Daniels, S.R., 2011. Reconstructing the colonisation and diversification history of the endemic freshwater crab (*Seychellum alluaudi*) in the granitic and volcanic Seychelles archipelago. *Mol Phylogenet Evol.* 61, 534–42. <https://doi.org/10.1016/j.ympev.2011.07.015>
- Dowling, H.G., 1990. Taxonomic status and relationships of the genus *Lycognathophis*. *Herpetologica* 1990, 60–66.
- Dowling, H.G., Duellman, W.E., 1978. *Systematic herpetology: a synopsis of families and higher categories*. New York: HISS Publications.
- Drummond A.J., Suchard, M.A., Xie, D., Rambaut, A., 2012. Bayesian phylogenetics with BEAUti and the BEAST 1.7 *Mol. Biol. Evol.* 29, 1969–1973. <https://doi.org/10.1093/molbev/mss075>
- Dubey, B., Meganathan, P.R., Vidal, N., Haque, I., 2012. Molecular evidence for the nonmonophyly of the Asian natricid genus *Xenochrophis* (Serpentes,

- Colubroidea) as inferred from mitochondrial and nuclear genes. *J. Herpetol.* 46(2), 263–269. <https://doi.org/10.1670/10-116>
- Felsenstein, J., 1981. Evolutionary trees from DNA sequences: a maximum likelihood approach. *J. Mol. Evol.* 17, 368–376. <https://doi.org/10.1007/BF01734359>
- Figuroa, A., McKelvy, A.D., Grismer, L.L., Bell, C.D., Lailvaux, S.P., 2016. A species-level phylogeny of extant snakes with description of a new colubrid subfamily and genus. *PLoS One*, 11(9), p.e0161070. <https://doi.org/10.1371/journal.pone.0161070>
- Gamble, T., Greenbaum, E., Russell, A.P., Jackman, T. R., Bauer, A.M., 2012. Repeated origin and loss of toepads in geckos. *PLoSOne* 7, e39429. <https://doi.org/10.1371/journal.pone.0039429>
- GBIF Global Biodiversity information Facility GBIF.org (accessed on 15 October 2019).
- Gerlach, J., Ineich, I., 2006. *Lycognathophis seychellensis*. The IUCN Red List of Threatened Species 2006: e.T61427A12481585. <https://doi.org/10.2305/IUCN.UK.2006.RLTS.T61427A12481585.en>
- Ganerød, M., Torsvik, T.H., van Hinsbergen, D.J.J., Gaina, C., Corfu, F., Werner, S., Owen-Smith, T.M., Ashwal, L.D., Webb, S.J., Hendriks, B.W.H., 2011. Palaeoposition of the Seychelles microcontinent in relation to the Deccan Traps and the Plume Generation Zone in Late Cretaceous-Early Palaeogene time. *Geological Society, London, Special Publications*, 357, 229–252.
- Gibbons, J.W., Dorcas, M.E., 2004. *North American Watersnakes: A Natural History (Animal Natural History Series)*. University of Oklahoma Press, Norman.

Gower, D.J., San Mauro, D., Giri, V., Bhatta, G., Govindappa, V., Kotharambath, R., Oommen, O.V., Fatih, F.A., Mackenzie-Dodds, J.A., Nussbaum, R.A., Biju, S.D., Shouche, Y.S., Wilkinson, M., 2011. Molecular systematics of caeciliid caecilians (Amphibia: Gymnophiona) of the Western Ghats, India. *Mol. Phylogenet. Evol.* 59(3), 698–707.

<https://doi.org/10.1016/j.ympev.2011.03.002>

Gower, D.J., Agarwal, I., Karanth, K.P., Datta- Roy, A., Giri, V.B., Wilkinson, M., San Mauro, D., 2016. The role of wet- zone fragmentation in shaping biodiversity patterns in peninsular India: insights from the caecilian amphibian

Gegeneophis. *J. Biogeogr.* 43(6),1091–1102. <https://doi.org/10.1111/jbi.12710>

Guo, P., Liu, Q., Xu, Y., Jiang, K., Hou, M., Ding, L., Pyron, R.A., Burbrink, F.T., 2012. Out of Asia: natricine snakes support the Cenozoic Beringian dispersal hypothesis. *Mol. Phylogenet. Evol.* 63(3), 825–833.

<https://doi.org/10.1016/j.ympev.2012.02.021>

Harris, D.J., Perera, A., Valente, J., Rocha, S., 2015. Deep genetic differentiation within *Janetaescincus* spp. (Squamata: Scincidae) from the Seychelles Islands. *Herpetol. J.* 25(4), 205–213.

Head, J.J., 2015. Fossil calibration dates for molecular phylogenetic analysis of snakes 1: serpentes, Alethinophidia, Boidae, Pythonidae. *Palaeontol.*

Electron. 18,1–17. <https://doi.org/10.26879/487>

Head, J.J., Mahlow, K., Müller, J., 2016. Fossil calibration dates for molecular phylogenetic analysis of snakes 2: caenophidia, Colubroidea, Elapoidea, Colubridae. *Palaeontol. Electron.* 19, 1–21.

- Janani, S.J., Vasudevan, K., Prendini, E., Dutta, S.K., Aggarwal, R.K., 2017. A new species of the genus *Nasikabatrachus* (Anura, Nasikabatrachidae) from the eastern slopes of the Western Ghats, India. *Alytes* 34, 1–19.
- Kamei, R.G., San Mauro, D., Gower, D.J., Van Bocxlaer, I., Sherratt, E., Thomas, A., Babu, S., Bossuyt, F., Wilkinson, M., Biju, S.D., 2012. Discovery of a new family of amphibians from northeast India with ancient links to Africa. *Proc. R. Soc. B.* 279, 2396–2401. <https://doi.org/10.1098/rspb.2012.0150>
- Kass, R.E., Raftery, A.E., 1995. Bayes factors. *J. Am. Statist. Assoc.* 90, 773–795.
- Kumar, S., Stecher, G., Tamura, K. 2016. MEGA7: Molecular Evolutionary Genetics Analysis version 7.0 for bigger datasets. *Mol. Biol. Evol.* 33, 1870–1874. <https://doi.org/10.1093/molbev/msy096>
- Labisko, J., Griffiths, R.A., Chong-Seng, L., Bunbury, N., Maddock, S.T., Bradfield, K.S., Taylor, M.L., Groombridge, J.J., 2019. Endemic, endangered and evolutionarily significant: cryptic lineages in Seychelles' frogs (Anura: Sooglossidae). *Biol. J. Linn. Soc.* 126(3) 417–435. <https://doi.org/10.1093/biolinnean/bly183>
- Lalronunga, S., Lalrinchhana, C., Vanramlina, Das, A., Gower, D.J., Deepak, V., 2020. A multilocus molecular perspective on the systematics of the poorly known Northeast Indian colubrid snakes *Blythia reticulata* (Blyth, 1854), *B. hmuifang* Vogel, Lalremsanga & Vanlalhrima, 2017, and *Hebius xenura* (Wall, 1907). *Zootaxa.* 4768(2), 193–200. <https://doi.org/10.11646/zootaxa.4768.2.2>
- Lanfear, R., Frandsen, P.B., Wright, A.M., Senfeld, T., Calcott, B., 2016. PartitionFinder 2: new methods for selecting partitioned models of evolution

for molecular and morphological phylogenetic analyses. *Mol. Biol. Evol.* 34(3), 772–773. <https://doi.org/10.1093/molbev/msw260>

Leigh, J.W., Bryant, D., 2015. Popart: full feature software for haplotype network construction. *Methods Ecol. Evol.* 6, 1110–1116. <https://doi.org/10.1111/2041-210X.12410>

Lima, A., Harris, D.J., Rocha, S., Miralles, A., Glaw, F., Vences, M., 2013. Phylogenetic relationships of *Trachylepis* skink species from Madagascar and the Seychelles (Squamata: Scincidae). *Mol. Phylogenet. Evol.* 67(3), 615–620. <https://doi.org/10.1016/j.ympev.2013.02.001>

Maddock, S.T., Day, J.J., Nussbaum, R.A., Wilkinson, M., Gower, D.J., 2014. Evolutionary origins and genetic variation of the Seychelles treefrog, *Tachycnemis seychellensis* (Duméril and Bibron, 1841) (Amphibia: Anura: Hyperoliidae). *Mol. Phylogenet. Evol.* 75, 194–201. <https://doi.org/10.1016/j.ympev.2014.02.004>

Maddock, S.T., Wilkinson, M., Nussbaum, R.A., Gower, D.J., 2017. A new species of small and highly abbreviated caecilian (Gymnophiona: Indotyphlidae) from the Seychelles island of Praslin, and a recharacterization of *Hypogeophis brevis* Boulenger, 1911. *Zootaxa* 4329, 301–326. <https://doi.org/10.11646/zootaxa.4329.4.1>

Maddock, S.T., Wilkinson, M., Gower, D.J., 2018. A new species of small, long-snouted *Hypogeophis* Peters, 1880 (Amphibia: Gymnophiona: Indotyphlidae) from the highest elevations of the Seychelles island of Mahé. *Zootaxa* 4450, 359–375. <https://doi.org/10.11646/zootaxa.4450.3.3>

Maddock, S.T., Nussbaum, R.A., Day, J.J., Latta, L., Miller, M., Wilkinson, M., Rocha, S., Gower, D.J., Pfrender, M.E., 2020. The roles of vicariance and

isolation by distance in shaping biotic diversification across an ancient archipelago: evidence from a Seychelles caecilian amphibian. *BMC Evol Biol* 20, 110. <https://doi.org/10.1186/s12862-020-01673-w>

Matzke, N.J., 2013. BioGeoBEARS: BioGeography with Bayesian (and likelihood) Evolutionary Analysis in R Scripts. Retrieved from <http://cran.r-project.org/web/packages/BioGeoBEARS/> (last accessed 14 October 2020).

Miller, M.A., Pfeiffer, W., Schwartz, T., 2010. Creating the CIPRES Science Gateway for inference of large phylogenetic trees. In: Proceedings of the Gateway Computing Environments Workshop (GCE), 14 Nov. 2010, New Orleans, LA, 1–8. <https://doi.org/10.1109/GCE.2010.5676129>

Minshull, T.A., Lane, C.I., Collier, J.S., Whitmarsh, R.B., 2008. The relationship between rifting and magmatism in the northeastern Arabian Sea. *Nat. Geosci.*, 1, 463–467.

Nagy, Z.T., Gvoždík, V., Meirte, D., Collet, M., Pauwels, O.S.G., 2014. New data on the morphology and distribution of the enigmatic Schouteden's sun snake, *Helophis schoutedeni* (de Witte, 1922) from the Congo Basin. *Zootaxa* 3755, 096–100. <https://doi.org/10.11646/zootaxa.3755.1.5>.

Nussbaum, R.A., 1984. Snakes of the Seychelles. In: D.R. Stoddart (Ed.), *Biogeography and Ecology of the Seychelles Islands*. W. Junk, The Hague. pp. 361–377.

Portik, D.M., Bell, R.C., Blackburn, D.C., Bauer, A.M., Barratt, C.D., Branch, W.R., Burger, M., Channing, A., Colston, T.J., Conradie, W., Dehling, J.M., Drewes, R.C., Ernst, R., Greenbaum, E., Gvoždík, V., Harvey, J., Hillers, A., Hirschfeld, M., Jongsma, G.F.M., Kielgast, J., Kouete, M.T., Lawson, L., Leaché, A.D., Loader, S.P., Lötters, S., van der Meijden, A., Menegon, M.,

- Müller, S., Nagy, Z.T., Ofori-Boateng, C., Ohler, A., Papenfuss, T.J., Rößler, D., Sinsch, U., Rödel, M.-O., Veith, M., Vindum, J., Zassi-Boulou, A.-G., McGuire, J.A., 2019. Sexual dichromatism drives diversification within a major radiation of African amphibians. *Syst. Biol.* 68(6), 859–875.
<https://doi.org/10.1093/sysbio/syz023>
- Pyron, R.A., Burbrink, F.T., Wiens, J.J., 2013. A phylogeny and revised classification of Squamata, including 4161 species of lizards and snakes. *BMC Evol. Biol.* 13(1), 93. <https://doi.org/10.1186/1471-2148-13-93>
- Quadros, A.B., Mahlow, K., Jalil, N.E., Zaher, H., 2019. Phylogenetic affinities of the fossil elapids *Naja romani* and *Naja antiqua* (Serpentes: Elapidae). *J. Morphol.* 280, S207.
- R Core Team., 2020. R: A language and environment for statistical computing. R Foundation for Statistical Computing, Vienna, Austria. <https://www.R-project.org/>.
- Rambaut, A., Suchard, M.A., Xie, D., Drummond, A.J., 2014. Tracer. Version 1.6. accessed 27 July 2018. <http://beast.bio.ed.ac.uk/Tracer/>
- Rambaut, A., 2016. FigTree (Tree Figure Drawing Tool) version 1.4.3 2006–2016. Institute of Evolutionary Biology, University of Edinburgh. Available at: accessed March 10, 2018. <http://tree.bio.ed.ac.uk/software/figtree/>
- Ree, R.H., Moore, B.R., Webb, C. O., Donoghue, M. J., 2005. A likelihood framework for inferring the evolution of geographic range on phylogenetic trees. *Evolution*, 59, 2299–2311. <https://doi.org/10.1111/j.0014-3820.2005.tb00940.x>

- Ree, R.H., Smith, S.A., Baker, A., 2008. Maximum likelihood inference of geographic range evolution by dispersal, local extinction, and cladogenesis. *Syst. Biol.*, 57, 4–14. <https://doi.org/10.1080/10635150701883881>
- Ree, R.H., Sanmartín, I., 2018. Conceptual and statistical problems with the DEC+J model of founder- event speciation and its comparison with DEC via model selection. *J. Biogeogr.*, 45, 741–749. <https://doi.org/10.1111/jbi.13173>
- Rocha, S., Rösler, H., Gehring, P-S., Glaw, F., Posada, D., Harris, D.J., Vences, M., 2010. Phylogenetic systematics of day geckos, genus *Phelsuma*, based on molecular and morphological data (Squamata: Gekkonidae). *Zootaxa* 2429, 1–28. <https://doi.org/10.5281/zenodo.194693>
- Rocha, S., Harris, D.J., Posada, D., 2011. Cryptic diversity within the endemic prehensile-tailed gecko *Urocytyledon inexpectata* across the Seychelles Islands: patterns of phylogeographical structure and isolation at the multilocus level. *Biol. J. Linn. Soc.* 104(1), 177–191. <https://doi.org/10.1111/j.1095-8312.2011.01710.x>
- Rocha, S., Posada, D., Harris, D.J., 2013. Phylogeography and diversification history of the day-gecko genus *Phelsuma* in the Seychelles islands. *BMC Evol. Biol.* 13(1), 3. <https://doi.org/10.1186/1471-2148-13-3>
- Rocha, S., Perera, A., Bunbury, N., Kaiser-Bunbury, C.N., Harris, D.J. 2016a. Speciation history and species-delimitation within the Seychelles bronze geckos, *Ailuronyx* spp.: molecular and morphological evidence. *Biol. J. Linn. Soc.* 120(3), 518–538. <https://doi.org/10.1111/bij.12895>
- Rocha, S., Perera, A., Silva, A., Posada, D., Harris, D.J., 2016b. Evolutionary history of *Trachylepis* skinks in the Seychelles islands: introgressive hybridization,

- morphological evolution and geographic structure. *Biol. J. Linn. Soc.* 119(1),15–36. <https://doi.org/10.1111/bij.12803>
- Ronquist, F., 1997. Dispersal-vicariance analysis: a new approach to the quantification of historical biogeography. *Syst. Biol.*, 46, 195–203.
- Ronquist, F., Sanmartín, I., 2011. Phylogenetic methods in biogeography. *Annu. Rev. Ecol. Evol. Syst.*, 42, 441–464. <https://doi.org/10.1146/annurev-ecolsys-102209-144710>.
- Ronquist, F., Teslenko, M., Van Der Mark, P., Ayres, D., Darling, A., Höhna, S., Larget, B., Liu, L., Suchard, M.A., Huelsenbeck, J.P., 2012. MrBayes 3.2: efficient Bayesian phylogenetic inference and model choice across a large model space. *Syst. Biol.* 61(3), 539–542. <https://doi.org/10.1093/sysbio/sys029>
- Samonds, K.E., Godfrey, L.R., Ali, J.R., Goodman, S.M., Vences, M., Sutherland, M.R., Irwin, M.T., Krause, D.W., 2012. Spatial and temporal arrival patterns of Madagascar's vertebrate fauna explained by distance, ocean currents, and ancestor type. *Proc. Natl. Acad. Sci.* 109(14), 5352–5357. <https://doi.org/10.1073/pnas.1113993109>.
- Sanderson, M.J., 2002. Estimating absolute rates of molecular evolution and divergence times: A penalized likelihood approach. *Mol. Biol. Evol.* 19, 101–109. <https://doi.org/10.1093/oxfordjournals.molbev.a003974>
- Shimodaira, H., 2002. An approximately unbiased test of phylogenetic tree selection. *Syst. Biol.* 51, 492–508. <https://doi.org/10.1080/10635150290069913>
- Shimodaira, H., Hasegawa, M., 1999. Multiple comparisons of loglikelihoods with applications to phylogenetic inference. *Mol. Biol. Evol.* 16, 1114–1116. <https://doi.org/10.1093/oxfordjournals.molbev.a026201>

- Shimodaira, H., Hasegawa, M., 2001. CONSEL: for assessing the confidence of phylogenetic tree selection. *Bioinformatics* 17, 1246–1247.
<https://doi.org/10.1093/bioinformatics/17.12.1246>
- Smith, S.A., O'Meara, B.C., 2012. treePL: divergence time estimation using penalized likelihood for large phylogenies. *Bioinformatics* 28(20), 2689–2690.
<https://doi.org/10.1093/bioinformatics/bts492>
- Stamatakis, A., 2006. RAxML-VI-HPC: maximum likelihood-based phylogenetic analyses with thousands of taxa and mixed models. *Bioinformatics* 22 (21), 2688–2690. <https://doi.org/10.1093/bioinformatics/btl446>
- Stamatakis, A., 2014. RAxML version 8: a tool for phylogenetic analysis and post-analysis of large phylogenies. *Bioinformatics* 30(9), 1312–1313.
<https://doi.org/10.1093/bioinformatics/btu033>.
- Swofford, D.L., 2000. PAUP*. Phylogenetic Analysis Using Parsimony (*and Other Methods). Version 4. Sinauer Associates, Sunderland, Massachusetts.
- Technelysium, P.L. 2012. Chromas Lite version 2.1. South Brisbane, Queensland, Australia.
- Thompson, J.D., Higgins, D.G., Gibson, T. J., 1994. ClustalW: improving the sensitivity of progressive multiple sequence alignment through sequence weighting, position-specific gap penalties and weight matrix choice. *Nucleic Acids Res.* 22, 4673–4680.
- Townsend, T.M., Tolley, K.A., Glaw, F., Böhme, W., Vences, M., 2010. Eastward from Africa: palaeocurrent-mediated chameleon dispersal to the Seychelles islands. *Biol. Lett.* 7(2), 225–228. <https://doi.org/10.1098/rsbl.2010.0701>

- Tolley, K.A., Townsend, T.M., Vences, M., 2013. Large-scale phylogeny of chameleons suggests African origins and Eocene diversification. *Proc. R. Soc. B.* 280(1759), 20130184. <https://doi.org/10.1098/rspb.2013.0184>
- Tsang, S.M., Wiantoro, S., Veluz, M.J., Sugita, N., Nguyen, Y.L., Simmons, N.B., Lohman, D.J. 2020. Dispersal out of Wallacea spurs diversification of *Pteropus* flying foxes, the world's largest bats (Mammalia: Chiroptera). *J. Biogeogr.*, 47(2), 527–537. <https://doi.org/10.1111/jbi.13750>
- Uetz, P., Freed, P., Hosek, J., 2020. The Reptile Database. Available from: accessed 8 November 2020. <http://reptile-database.reptarium.cz/>
- Valente, J., Rocha, S., Harris, D.J., 2014. Differentiation within the endemic burrowing skink *Pamelaescincus gardineri*, across the Seychelles islands, assessed by mitochondrial and nuclear markers. *Afr. J. Herpetol.*, 63(1), 25–33. <https://doi.org/10.1080/21564574.2013.856354>
- Vidal, N., Branch, W.R., Pauwels, O.S., Hedges, S.B., Broadley, D.G., Wink, M., Cruaud, C., Joger, U., Nagy, Z.T., 2008. Dissecting the major African snake radiation: a molecular phylogeny of the Lamprophiidae Fitzinger (Serpentes, Caenophidia). *Zootaxa* 1945, 51–66. <https://doi.org/10.11646/zootaxa.1945.1.3>
- Vitt, L.J., Caldwell, J.P., 2009. *Herpetology*. Elsevier, Burlington, MA.
- Warren, B.H., Dominique, S., Bruggemann, J.H., Robert, P.P-J., Christophe, T., 2010. Why does the biota of the Madagascar region have such a strong Asiatic flavour? *Cladistics* 26, 526–538. <https://doi.org/10.1111/j.1096-0031.2009.00300.x>

- Warren, D.L., Geneva, A.J., Lanfear, R., 2017. RWTY (R We There Yet): An R package for examining convergence of Bayesian phylogenetic analyses. *Mol. Biol. Evol.* 34,1016–1020. <https://doi.org/10.1093/molbev/msw279>
- Weinell, J.L., Branch, W.R., Colston, T.J., Jackman, T.R., Kuhn, A., Conradie, W., Bauer, A.M., 2019. A species-level phylogeny of *Trachylepis* (Scincidae: Mabuyinae) provides insight into their reproductive mode evolution. *Mol. Phylogenet. Evol.* 136, 183–195. <https://doi.org/10.1016/j.ympev.2019.04.002>
- Wiens, J.J., Kuczynski, C.A., Smith, S.A., Mulcahy, D.G., Sites Jr, J.W., Townsend, T.M., Reeder, T.W., 2008. Branch lengths, support, and congruence: testing the phylogenomic approach with 20 nuclear loci in snakes. *Syst. Biol.* 57(3), 420–431. <https://doi.org/10.1080/10635150802166053>
- Wilkinson, M., Sheps, J.A., Oommen, O.V., Cohen, B.L., 2002. Phylogenetic relationships of Indian caecilians (Amphibia: Gymnophiona) inferred from mitochondrial rRNA gene sequences. *Mol. Phylogenet. Evol.* 23(3), 401–407. [https://doi.org/10.1016/s1055-7903\(02\)00031-3](https://doi.org/10.1016/s1055-7903(02)00031-3)
- Williams, R., Gower, D.J., Labisko, J., Morel, C., Bristol, R.M., Wilkinson, M., Maddock, S.T. 2020. Are the Mascarene frog (*Ptychadena mascareniensis*) and Brahminy blind snake (*Indotyphlops braminus*) really alien species in the Seychelles? *Herpetol. Bull.*, 153: 17–21. <https://doi.org/10.33256/hb153.1721>
- Witte, G.F. de., 1922. Description d'un ophidien nouveau récolté au Congo par le Dr. Schouteden. *Rev. Zool. Afric.*, 10, 318–319.
- Zaher, H., Murphy, R.W., Arredondo, J.C., Graboski, R., Machado-Filho, P.R., Mahlow, K., Montingelli, G.G., Quadros, A.B., Orlov, N.L., Wilkinson, M., Zhang, Y.P., Grazziotin F.G., 2019. Large-scale molecular phylogeny, morphology, divergence-time estimation and the fossil record of advanced

caenophidian snakes (Squamata: Serpentes). PLoS One, 14(5), e0216148.

<https://doi.org/10.1371/journal.pone.0216148>

Table 1. Sequences generated in this study. Sequences used in the 21-leaf dataset are indicated with *, en-dash (–) = no data, different Islands in Seychelles are marked bold.

| Sampl e | Species | voucher number/extracti on ID | Latitude | Longitud e | Sequenc e ID | Location | 16s | cytb | nd4 | cmos | nt3 | bdnf | rag1 | prlr |
|------------|---------------------------------------|-------------------------------------|-----------|---------------------|-----------------|--|----------|----------|----------|----------|--------------|--------------|--------------|------|
| 1 | <i>Afronatrix anoscopus*</i> | NHMUK 2013:383 | 6.05370 | 9.47322 | AE-40 | Akwa, Mamfe division, Cameroon | MW699965 | MW711484 | – | MW711535 | MW71145 2 | MW71155 8 | MW71158 9 | – |
| 2 | <i>Afronatrix anoscopus*</i> | Lake Kuk, Cameroon | 6.41072 | 10.2081 2 | AE-41 | LakeKuk, Cameroon Mount Nimba mining concession, Forestiere Region, Guinea | MW699966 | MW711485 | – | MW711536 | MW71145 3 | MW71155 9 | MW71159 0 | – |
| 3 | <i>Afronatrix anoscopus*</i> | BMNH2008.637 | 7.69960 | -8.39880 22.7869 | AE-42 | Guinea | MW699967 | MW711486 | MW711522 | MW711537 | – | MW71156 0 | MW71159 1 | – |
| 4 | <i>Helophis schoutedeni*</i> | CRT3853 | 2.03306 | 22.7869 4 | AI-89 | DR Congo, Kona | MW699968 | – | MW711523 | MW711538 | MW71145 4 | MW71156 1 | MW71159 2 | – |
| 5 | <i>Helophis schoutedeni*</i> | CRT3855 | 2.03306 | 22.7869 4 | AJ-90 | DR Congo, Kona | MW699969 | – | MW711524 | MW711539 | MW71145 5 | MW71156 2 | MW71159 3 | – |
| 6 | <i>Helophis schoutedeni</i> | CRT3859 | 2.03306 | 22.7869 4 | AJ-91 | DR Congo, Kona | MW699970 | – | – | MW711540 | MW71145 6 | MW71156 3 | – | – |
| 7 | <i>Helophis schoutedeni</i> | CRT3860 | 2.03306 | 22.7869 4 | AJ-92 | DR Congo, Kona | MW699971 | – | – | MW711541 | MW71145 7 | MW71156 4 | – | – |
| 8 | <i>Hydraethiops melanogaster*</i> | NMP-P6V 75763 | 1.05000 | 26.8300 0 | AI-84 | Bafwabianga village, DR Congo | MW699972 | – | MW711525 | MW711542 | MW71145 8 | MW71156 5 | MW71159 4 | – |
| 9 | <i>Hydraethiops melanogaster</i> | NMP-P6V 75491 | 0.54000 | 12.8300 0 | AI-85 | Makokou, Gabon | MW699973 | – | MW711526 | MW711543 | MW71145 9 | MW71156 6 | MW71159 5 | – |
| 10 | <i>Hydraethiops melanogaster*</i> | NMP-P6V 75772 | 1.81000 | 14.5500 0 | AI-86 | Dia near Sembe, Congo Rep. | MW699974 | – | MW711527 | MW711544 | MW71146 0 | MW71156 7 | MW71159 6 | – |
| 11 | <i>Limnophis bangweolicus*</i> | ANG-438 | -17.57333 | 23.2266 7 | AI-82 | West of Sashae, Cuando Cubango, Angola | MT586815 | MT587279 | MT587306 | MT587292 | MW71146 1 | MW71156 8 | MW71159 7 | – |
| 12 | <i>Limnophis bicolor*</i> | WC-6238 | -12.33012 | 18.4047 9 | AI-83 | upstream of Lungue- bungue River bridge, Moxico, Angola | MT586817 | MT587281 | MT587307 | MT587294 | MW71146 2 | MW71156 9 | MW71159 8 | – |
| 13 | <i>Limnophis branchi</i> | ANG-056 | -7.75308 | 19.9568 6 | AI-80 | Lulele River area, Lunda Norte, Angola | MT586818 | MT587283 | MT587308 | MT587296 | MW71146 3 | MW71157 0 | MW71159 9 | – |
| 14 | <i>Limnophis branchi</i> | ANG-058 | -7.75308 | 19.9568 6 | AI-81 | Lulele River area, Lunda Norte, Angola | MT586819 | MT587284 | MT587309 | MT587297 | MW71146 4 | MW71157 1 | MW71160 0 | – |
| 15 | <i>Natriciteres fuliginoides*</i> | CAS258133 | -0.05171 | 11.1662 1 | AD-33 | Moyen-Ogooue Prov., Gabon | MW699975 | MW711487 | MW711528 | MW711545 | MW71146 5 | MW71157 2 | MW71160 1 | – |
| 16 | <i>Natriciteres olivacea*</i> | CAS220640 | – | – | AD-34 | DR Congo | MT586821 | MT587285 | MT587311 | MT587299 | MW71146 6 | MW71157 3 | – | – |
| 17 | <i>Natriciteres olivacea*</i> | WRB-636 | -5.93333 | 29.2000 0 | AI-87 | Kalemie, DR Congo Udzungwa Mts., Uzungwa Scarp F. R., Mkalazi, Tanzania | MW699976 | MW711488 | MW711529 | MW711546 | MW71146 7 | MW71157 4 | MW71160 2 | – |
| 18 | <i>Natriciteres sylvatica*</i> | MTSN5485 | -8.39750 | 35.9786 1 | AD-36 | Nguru South Mts., (Pemba), Tanzania | MW699977 | MW711489 | MW711530 | MW711547 | MW71146 8 | MW71157 5 | MW71160 3 | – |
| 19 | <i>Natriciteres sylvatica</i> | MTSN8183 | -6.03044 | 37.5256 4 | AD-37 | MW699978 | | MW711490 | – | – | – | – | – | – |

| Sample | Species | voucher number/extract ID | Latitude | Longitude | Sequence ID | Location | 16s | cytb | nd4 | cmos | nt3 | bdnf | rag1 | prlr |
|--------|---------------------------------------|---------------------------|-----------|-----------|-------------|---|----------|----------|----------|----------|----------|----------|----------|----------|
| 20 | <i>Natriciteres sylvatica</i> * | MUSE13712 | - | - | AD-38 | Rungwe Mt. (Nkuka), Southern Highlands, Tanzania | MW699979 | MW711491 | MW711531 | MW711548 | MW711469 | MW711576 | MW711604 | - |
| 21 | <i>Natriciteres sylvatica</i> | WRB-642 | -16.28789 | 36.41244 | AI-88 | Mount Mabu, Zambezi, Mozambique | MW699980 | MW711492 | MW711532 | MW711549 | - | MW711577 | - | - |
| 22 | <i>Natriciteres variegata</i> | MUSE13726 | - | - | AD-39 | Rungwe Mt. (Nkuka), Southern Highlands, Tanzania | MW699981 | - | - | - | - | - | - | - |
| 23 | <i>Fowlea flavipunctatus</i> * | FMNH250122 | - | - | AC-21 | Thailand | MT586822 | MT587286 | MT587312 | MT587300 | MW711470 | MW711578 | MW711605 | - |
| 24 | <i>Amphiesma stolatum</i> * | CAS213646 | 20.31286 | 94.74683 | AC-29 | Myanmar | MT586823 | MT587287 | MT587313 | MT587301 | MW711471 | MW711579 | MW711606 | - |
| 25 | <i>Rhabdops olivaceus</i> | NCBS-AU164 | 11.53932 | 76.02188 | | Pookode, Wayanad District, Kerala, India | MF352831 | MF352838 | MF352842 | MF352834 | MW711472 | MW711580 | MW711607 | - |
| 26 | <i>Smithophis atemporalis</i> | BNHS 3527 | 23.76338 | 93.09916 | | Mizoram University Campus, Aizawl, Mizoram, India | MK350255 | MK350262 | MK350258 | MK350265 | MW711473 | MW711581 | MK350257 | - |
| 27 | <i>Smithophis bicolor</i> | BNHS 2369 | 23.71083 | 92.93194 | | Mizoram University Campus, Aizawl, Mizoram, India | MK350254 | MK350261 | MK350259 | MK350264 | MW711474 | MW711582 | MK350256 | - |
| 28 | <i>Lycognathophis seychellensis</i> | SM251 | -4.65894 | 55.43744 | | Morne Blanc Trail, Mahé, Seychelles | MW699982 | MW711493 | - | - | MW711475 | - | - | MW711610 |
| 29 | <i>Lycognathophis seychellensis</i> * | SM165 | -4.63738 | 55.41212 | AM-126 | Mare Aux Cochons, Mahé, Seychelles | MW699983 | MW711494 | MW711533 | MW711550 | MW711476 | MW711583 | MW711608 | - |
| 30 | <i>Lycognathophis seychellensis</i> | SM252 | -4.65350 | 55.43778 | | Casse Dent, Mahé, Seychelles | MW699984 | MW711495 | - | - | - | - | - | MW711611 |
| 31 | <i>Lycognathophis seychellensis</i> | SM286 | -4.64493 | 55.43363 | | Congo Rouge, Mahé, Seychelles | MW699985 | MW711496 | - | MW711551 | MW711477 | MW711584 | - | MW711612 |
| 32 | <i>Lycognathophis seychellensis</i> | SM287 | -4.65043 | 55.43765 | | Congo Rouge, Mahé, Seychelles | MW699986 | MW711497 | - | - | - | - | - | - |
| 33 | <i>Lycognathophis seychellensis</i> | SM290 | - | - | | Mahé, Seychelles | MW699987 | MW711498 | - | - | - | - | - | MW711613 |
| 34 | <i>Lycognathophis seychellensis</i> | R9458 | -4.63487 | 55.41158 | | Mare Aux Cochons, Mahé, Seychelles | MW699988 | - | - | - | - | - | - | - |
| 35 | <i>Lycognathophis seychellensis</i> | R6716 | -4.70760 | 55.50081 | | La Reserve, Mahé, Seychelles | MW699989 | - | - | - | - | - | - | MW711614 |
| 36 | <i>Lycognathophis seychellensis</i> | R6909 | -4.65716 | 55.43421 | | Trail to Morne Blanc, Mahé, Seychelles | MW699990 | MW711499 | - | - | - | - | - | MW711615 |
| 37 | <i>Lycognathophis seychellensis</i> | SM292 | -4.64007 | 55.41602 | | Mare Aux Cochons, Mahé, Seychelles | MW699991 | MW711500 | - | MW711552 | - | - | - | MW711616 |
| 38 | <i>Lycognathophis seychellensis</i> | SM293 | -4.62853 | 55.41139 | | Mare Aux Cochons, Mahé, Seychelles | MW699992 | MW711501 | - | - | MW711478 | - | - | - |
| 39 | <i>Lycognathophis seychellensis</i> | SM339 | -4.64883 | 55.42858 | | Between Mare Aux Cochons and Casse Dent, Mahé, Seychelles | MW699993 | MW711502 | - | - | - | - | - | MW711617 |
| 40 | <i>Lycognathophis seychellensis</i> | SM340 | -4.65114 | 55.41194 | | Between Mare Aux Cochons and Casse Dent, Mahé, Seychelles | MW699994 | MW711503 | - | - | - | - | - | MW711618 |
| 41 | <i>Lycognathophis seychellensis</i> | SM385 | -4.64675 | 55.43450 | | Congo Rouge trail, Mahé, Seychelles | MW699995 | MW711504 | - | - | - | - | - | MW711619 |

| Sample | Species | voucher number/extraction ID | Latitude | Longitude | Sequence ID | Location | 16s | cytb | nd4 | cmos | nt3 | bdnf | rag1 | prlr |
|--------|-------------------------------------|------------------------------|----------|-----------|-------------|---|----------|----------|----------|----------|----------|----------|----------|----------|
| 42 | <i>Lycognathopsis seychellensis</i> | SM87 | -4.33180 | 55.73885 | | Vallée de Mai, Praslin , Seychelles | MW699996 | MW711505 | - | - | - | - | - | MW711620 |
| 43 | <i>Lycognathopsis seychellensis</i> | SM88 | -4.33180 | 55.73885 | | Vallée de Mai, Praslin , Seychelles | MW699997 | MW711506 | - | - | - | - | - | MW711621 |
| 44 | <i>Lycognathopsis seychellensis</i> | SM89 | -4.33077 | 55.73763 | | Vallée de Mai, Praslin , Seychelles | MW699998 | MW711507 | - | MW711553 | - | - | - | - |
| 45 | <i>Lycognathopsis seychellensis</i> | SM112 | -4.30359 | 55.69084 | | Anse Kerlan River, Praslin , Seychelles | MW699999 | MW711508 | - | - | - | - | - | MW711622 |
| 46 | <i>Lycognathopsis seychellensis</i> | R9459 | -4.33475 | 55.73384 | | Praslin , Seychelles | MW700000 | - | - | - | - | - | - | MW711623 |
| 47 | <i>Lycognathopsis seychellensis</i> | R9469 | -4.33143 | 55.73762 | | Vallée de Mai, Praslin , Seychelles | MW700001 | MW711509 | - | - | - | - | - | MW711624 |
| 48 | <i>Lycognathopsis seychellensis</i> | SM206 | -4.48528 | 55.23781 | | Trail to Jardin Maron, Silhouette , Seychelles | MW700002 | MW711510 | - | - | - | - | - | - |
| 49 | <i>Lycognathopsis seychellensis</i> | SM213 | -4.47890 | 55.24621 | AM-127 | Hotel Hilton LeBreeze, Silhouette , Seychelles | MW700003 | MW711511 | MW711534 | MW711554 | MW711479 | MW711585 | MW711609 | MW711625 |
| 50 | <i>Lycognathopsis seychellensis</i> | SM225 | -4.48474 | 55.23967 | | Trail to Jardin Maron, Silhouette , Seychelles | MW700004 | MW711512 | - | MW711555 | MW711480 | MW711586 | - | - |
| 51 | <i>Lycognathopsis seychellensis</i> | R9467 | -4.48450 | 55.24260 | | Silhouette , Seychelles | MW700005 | - | - | - | - | - | - | - |
| 52 | <i>Lycognathopsis seychellensis</i> | R6680 | -4.48704 | 55.23544 | | Trail to Jardin Maron, Silhouette , Seychelles | MW700006 | MW711513 | - | - | - | - | - | MW711626 |
| 53 | <i>Lycognathopsis seychellensis</i> | R6723 | -4.48497 | 55.23800 | | Trail to Jardin Maron, Silhouette , Seychelles | MW700007 | MW711514 | - | - | - | - | - | MW711627 |
| 54 | <i>Lycognathopsis seychellensis</i> | R9460 | -4.35872 | 55.84062 | | Belle Vue, La Digue , Seychelles | MW700008 | MW711515 | - | - | - | - | - | - |
| 55 | <i>Lycognathopsis seychellensis</i> | R9464 | -4.37145 | 55.82741 | | Anse Source d'Argent, La Digue , Seychelles | MW700009 | MW711516 | - | MW711556 | MW711481 | MW711587 | - | - |
| 56 | <i>Lycognathopsis seychellensis</i> | R9465 | -4.58581 | 55.94387 | | Frégate , Seychelles | MW700010 | MW711517 | - | MW711557 | MW711482 | MW711588 | - | - |
| 57 | <i>Lycognathopsis seychellensis</i> | R9466 | -4.58581 | 55.94387 | | Frégate , Seychelles | MW700011 | MW711518 | - | - | MW711483 | - | - | MW711628 |
| 58 | <i>Lycognathopsis seychellensis</i> | SM505 | -4.58475 | 55.93317 | | Frégate , Seychelles | - | MW711519 | - | - | - | - | - | - |
| 59 | <i>Lycognathopsis seychellensis</i> | SM506 | -4.58475 | 55.93317 | | Frégate , Seychelles | - | MW711520 | - | - | - | - | - | MW711629 |
| 60 | <i>Lycognathopsis seychellensis</i> | SM507 | -4.58475 | 55.93317 | | Frégate , Seychelles | - | MW711521 | - | - | - | - | - | MW711630 |

Table 2. GenBank accession and voucher numbers for gene sequences used in molecular dating analysis. – = no data

| Sample | Species | Family | Sequence ID | 16s | cytb | nd4 | cmos | nt3 | bdnf | rag1 (part 'a') | rag1 (part 'b') |
|--------|---------------------------------|-------------------------------------|-------------|----------|----------|----------|----------|----------|----------|-----------------|-----------------|
| 1 | <i>Acrochordus granulatus</i> | Acrochordidae | | AF544786 | AF217841 | HM234054 | HM234057 | FJ434082 | FJ433981 | – | – |
| 2 | <i>Acrochordus javanicus</i> | Acrochordidae | | AF512745 | KX694897 | HM234055 | HM234058 | KX694991 | AY988036 | – | HM234061 |
| 3 | <i>Afronatrix anoscopus</i> | Colubridae (Natricinae) | AE 41 | MW699966 | MW711485 | – | MW711536 | MW711453 | MW711559 | MW711590 | – |
| 4 | <i>Afronatrix anoscopus</i> | Colubridae (Natricinae) | AE 42 | MW699967 | MW711486 | MW711522 | MW711537 | – | MW711560 | MW711591 | – |
| 5 | <i>Agkistrodon contortrix</i> | Viperidae (Crotalinae) | | AF156566 | EU483383 | AF156577 | – | – | EU402623 | – | EU402833 |
| 6 | <i>Ahaetulla pulverulenta</i> | Colubridae (Ahaetuliinae) | | KC347339 | KC347454 | KC347512 | KC347378 | – | – | – | KC347416 |
| 7 | <i>Anilius scytale</i> | Aniliidae | | FJ755180 | U69738 | FJ755180 | AF544722 | FJ434066 | EU402625 | – | AY988072 |
| 8 | <i>Anomochilus leonardi</i> | Cylindrophiidae+Anomochiliidae | | AY953431 | – | – | – | – | – | – | – |
| 9 | <i>Aparallactus capensis</i> | Atractaspididae (Aparallactinae) | | AY188045 | AY188006 | FJ404331 | AY187967 | – | – | – | – |
| 10 | <i>Aplopeltura boa</i> | Pareidae (Pareinae) | | AF544787 | JF827673 | JF827650 | JF827696 | FJ434085 | FJ433984 | – | – |
| 11 | <i>Aspidura ceylonensis</i> | Colubridae (Natricinae) | | KC347361 | KC347477 | KC347527 | KC347400 | – | – | – | KC347438 |
| 12 | <i>Asthenodipsas malaccanus</i> | Pareidae (Pareinae) | | KX660197 | KX660469 | KX660597 | KX660336 | – | – | – | – |
| 13 | <i>Azemiope feae</i> | Viperidae (Azemiopinae) | | AF057234 | AY352747 | AY352808 | AF544695 | KX694977 | EU402628 | – | EU402836 |
| 14 | <i>Bitis nasicornis</i> | Viperidae (Viperinae) | | AY188048 | DQ305457 | DQ305475 | AY187970 | – | – | – | KC330012 |
| 15 | <i>Boa constrictor</i> | Boidae | | AB177354 | AB177354 | AB177354 | AF544676 | – | KC330044 | – | KC347423 |
| 16 | <i>Boaedon fuliginosus</i> | Lamprophiidae (Lamprophiinae) | | AY188079 | AF471060 | FJ404365 | FJ404270 | FJ434094 | EU402646 | KM519732 | EU402849 |
| 17 | <i>Bothrolycus ater</i> | Lamprophiidae (Lamprophiinae) | | AY611859 | AY612041 | AY611950 | FJ404347 | – | – | – | – |
| 18 | <i>Bufo depressiceps</i> | Lamprophiidae <i>incertae sedis</i> | | AY611860 | AY612042 | – | AY611951 | – | – | – | – |
| 19 | <i>Bufo procterae</i> | Lamprophiidae <i>incertae sedis</i> | | AY611818 | AY612001 | DQ486328 | AY611910 | – | – | – | – |
| 20 | <i>Bungarus fasciatus</i> | Elapidae | | EU579523 | EU579523 | EU579523 | AY058924 | KX694998 | FJ433989 | JF357954 | – |
| 21 | <i>Calabaria reinhardtii</i> | Calabariidae | | Z46494 | AY099985 | – | AF544682 | – | EU402631 | – | EU402839 |
| 22 | <i>Calamaria pavimentata</i> | Colubridae (Calamariinae) | | KX694624 | AF471081 | – | AF471103 | KX694999 | FJ434005 | – | – |
| 23 | <i>Candoia carinata</i> | Candoiidae | | EU419850 | AY099984 | – | AY099961 | FJ434077 | FJ433974 | – | AY988065 |
| 24 | <i>Cantoria violacea</i> | Homalopsidae | | KX694627 | EF395897 | EF395922 | – | KX695001 | KX694704 | – | – |

| Sampl e | Species | Family | Sequenc e ID | 16s | cytb | nd4 | cmos | nt3 | bdnf | rag1 (part 'a') | rag1 (part 'b') |
|------------|-------------------------------------|------------------------------------|-----------------|----------|----------|----------|----------|----------|----------|--------------------|--------------------|
| 25 | <i>Casarea dussumieri</i> | Bolyeridae | | AF544827 | U69755 | – | AF544731 | FJ434069 | EU402632 | – | EU402840 |
| 26 | <i>Charina bottae</i> | Charinidae (Charininae) | | AF544816 | AY099986 | AF302959 | AY099971 | FJ434079 | FJ433978 | – | AY988076 |
| 27 | <i>Chilabothrus striatus</i> | Boidae | | – | – | KC329966 | KC329991 | DQ465554 | KC330056 | – | KC330027 |
| 28 | <i>Contia tenuis</i> | Colubridae (Dipsadinae) | | AY577030 | GU112384 | GU112419 | AF471134 | – | GU112346 | – | – |
| 29 | <i>Corallus annulatus</i> | Boidae | | – | KC750012 | KC750018 | KC750007 | – | JX576167 | – | KC750047 |
| 30 | <i>Cylindrophis ruffus</i> | Cylindrophidae+Anomochilidae | | AB179619 | AB179619 | AB179619 | AF471133 | – | AY988037 | AY662613 | AY988071 |
| 31 | <i>Daboia russellii</i> | Viperidae (Viperinae) | | EU913478 | EU913478 | EU913478 | AF471156 | – | EU402636 | – | EU402843 |
| 32 | <i>Dityopphis vivax</i> | Lamprophiidae | | – | – | – | – | – | JQ073079 | – | JQ073200 |
| 33 | <i>Epicrates cenchria</i> | Boidae | | – | HQ399501 | KC329975 | KC330008 | JX576186 | KC330073 | – | – |
| 34 | <i>Eryx colubrinus</i> | Erycidae | | AF544819 | U69811 | – | AF544716 | DQ465569 | EU402639 | – | DQ465571 |
| 35 | <i>Eryx conicus</i> | Erycidae | | AF512743 | GQ225658 | GQ225672 | – | – | – | – | AY988074 |
| 36 | <i>Eunectes notaeus</i> | Boidae | | AM236347 | HQ399499 | KC329978 | HQ399536 | – | KC330076 | – | HQ399516 |
| 37 | <i>Gerrhopilus mirus</i> | Gerrhopilidae | | AM236345 | AM236345 | AM236345 | – | GU902566 | GU902394 | – | – |
| 38 | <i>Grayia ornata</i> | Colubridae (Grayiinae) | | AY611866 | AY612048 | AF544663 | AF544684 | KX695019 | FJ434002 | – | – |
| 39 | <i>Helophis schoutedeni</i> | Colubridae (Natricinae) | AI 89 | MW699968 | – | MW711523 | MW711538 | MW711454 | MW711561 | MW711592 | – |
| 40 | <i>Hologerrhum philippinum</i> | Lamprophiidae (Cyclocorinae) | | – | MG458758 | – | MG458766 | – | – | – | – |
| 41 | <i>Homoroselaps lacteus</i> | Lamprophiidae (Atractaspidinae) | | AY611809 | AY611992 | FJ404338 | AY611901 | KX695021 | JQ599029 | MK621524 | – |
| 42 | <i>Hydraethiops melanogaster</i> | Colubridae (Natricinae) | AI 84 | MW699972 | – | MW711525 | MW711542 | MW711458 | MW711565 | MW711594 | – |
| 43 | <i>Liasis mackloti</i> | Pythonidae | | EF545051 | U69839 | – | AF544726 | FJ434075 | FJ433959 | – | – |
| 44 | <i>Limnophis bangweolicus</i> | Colubridae (Natricinae) | AI 82 | MT586815 | MT587279 | MT587306 | MT587292 | MW711461 | MW711568 | MW711597 | – |
| 45 | <i>Limnophis branchi</i> | Colubridae (Natricinae) | AI 81 | MT586819 | MT587284 | MT587309 | MT587297 | MW711464 | MW711571 | MW711600 | – |
| 46 | <i>Liopholidophis sexlineatus</i> | Lamprophiidae (Pseudoxyrhophiinae) | | AY188063 | DQ979985 | FJ404373 | AY187985 | – | – | – | – |
| 47 | <i>Liotyphlops albirostris</i> | Anomalepididae | | AF366762 | AF544672 | – | AF544727 | – | EU402650 | – | – |
| 48 | <i>Loxocemus bicolor</i> | Loxocemidae | | AF544828 | AY099993 | – | AY444035 | FJ434072 | EU402651 | – | – |
| 49 | <i>Lycognathophis seychellensis</i> | Colubridae (Natricinae) | AM 126 | MW699983 | MW711494 | MW711533 | MW711550 | MW711476 | MW711583 | MW711608 | – |
| 50 | <i>Micrelaps bicoloratus</i> | Lamprophiidae (Aparallactinae) | | – | DQ486349 | – | DQ486173 | – | – | – | – |

| Sampl e | Species | Family | Sequenc e ID | 16s | cytb | nd4 | cmos | nt3 | bdnf | rag1 (part 'a') | rag1 (part 'b') |
|------------|--|------------------------------------|-----------------|----------|----------|----------|----------|----------|---------------|--------------------|--------------------|
| 51 | <i>Mimophis mahfalensis</i> | Lamprophiidae (Psammophiinae) | | AY188070 | DQ486461 | – | AY187992 | KX695030 | JQ073081 | – | – |
| 52 | <i>Naja (Afronaja) mossambica</i> | Elapidae | | AY611813 | AY611996 | DQ897723 | AY611905 | – | – | – | – |
| 53 | <i>Naja (Boulengerina) melanoleuca</i> | Elapidae | | AY611812 | AY611995 | KX130765 | AY611904 | – | – | – | – |
| 54 | <i>Natriciteres fuliginoides</i> | Colubridae (Natricinae) | AD 33 | MW699975 | MW711487 | MW711528 | MW711545 | MW711465 | MW711572 | MW711601 | – |
| 55 | <i>Natriciteres olivacea</i> | Colubridae (Natricinae) | AI 87 | MW699976 | MW711488 | MW711529 | MW711546 | MW711467 | MW711574 | MW711602 | – |
| 56 | <i>Natriciteres sylvatica</i> | Colubridae (Natricinae) | AD 36 | MW699977 | MW711489 | MW711530 | MW711547 | MW711468 | MW711575 | MW711603 | – |
| 57 | <i>Oxyrhabdium leporinum</i> | Lamprophiidae (Cyclocorinae) | | – | AF471029 | – | DQ112081 | – | – | – | – |
| 58 | <i>Oxyuranus scutellatus</i> | Elapidae | | EU547149 | EU547051 | EF210827 | EU546916 | – | – | EU546877 | – |
| 59 | <i>Pareas carinatus</i> | Pareidae (Pareinae) | | AF544802 | JF827677 | JF827653 | JF827702 | FJ434086 | FJ433985 | – | – |
| 60 | <i>Prosymna janii</i> | Lamprophiidae (Prosymninae) | | FJ404222 | FJ404319 | FJ404389 | FJ404293 | – | – | – | – |
| 61 | <i>Pseudaspis cana</i> | Lamprophiidae (Pseudaspidinae) | | AY611898 | AY612080 | DQ486319 | DQ486167 | – | – | – | – |
| 62 | <i>Pseudoxenodon karlschmidti</i> | Colubridae (Pseudoxenodontinae) | | JF697330 | AF471080 | – | AF471102 | KX695042 | JQ599045 | – | – |
| 63 | <i>Python bivittatus</i> | Pythonidae | | KF010492 | JX401131 | – | AF435016 | | XM743302 2 | XM – 007441886 | – |
| 64 | <i>Rhinophis drummondhayi</i> | Uropeltidae | | AY701028 | AF544673 | – | AF544719 | FJ434071 | FJ433966 | – | – |
| 65 | <i>Sanzinia madagascariensis</i> | Sanziniidae | | AY336066 | U69866 | – | EU403580 | – | AY988033 | – | AY988067 |
| 66 | <i>Sibynophis subpunctatus</i> | Colubridae (Sibynophiinae) | | KC347373 | KC347471 | KC347516 | KC347411 | – | – | – | KC347449 |
| 67 | <i>Tropidophis feicki</i> | Tropidophiidae | | AF512733 | KF811124 | – | KF811110 | – | KF811074 | – | – |
| 68 | <i>Ungaliophis continentalis</i> | Charinidae (Ungaliophiinae) | | AF544833 | U69870 | – | AF544724 | FJ434081 | EU402665 | – | EU402867 |
| 69 | <i>Fowlea flavipunctatus</i> | Colubridae (Natricinae) | AC 21 | MT586822 | MT587286 | MT587312 | MT587300 | MW711470 | MW711578 | MW711605 | – |
| 70 | <i>Xenodermus javanicus</i> | Xenodermidae | | AF544810 | – | U49320 | AF544711 | – | EU402667 | – | EU402869 |
| 71 | <i>Xenopeltis unicolor</i> | Xenopeltidae | | AB179620 | AB179620 | AB179620 | AF544689 | FJ434073 | EU402668 | – | DQ465564 |
| 72 | <i>Xenophidion schaeferi</i> | Xenophidiidae | | – | AY574279 | – | – | – | – | – | – |
| 73 | <i>Xylophis perroteti</i> | Pareidae (Xylophiinae) | | MK340908 | – | MK340910 | MK344193 | – | MK344197 | – | MK340913 |

Table 3. Quantitative support (ML bootstrap and Bayesian posterior probability values) for three incompatible clades, representing the three best supported resolutions of the relationships of *Lycognathophis seychellensis* under ML and BI analyses of the 21-leaf, concatenated mt and nu dataset. Values in bold indicate best-supported resolution for each analysis. Abbreviations of genera: *Af* = *Afronatrix*; *He* = *Helophis*; *Hy* = *Hydraethiops*; *Li* = *Limnophis*; *Ly* = *Lycognathophis*; *Na* = *Natriciteres*.

| Analysis | (<i>Ly</i> (<i>Hy</i> , <i>He</i> , <i>Af</i>)) | ((<i>Na</i> , <i>Li</i>)(<i>Hy</i> , <i>He</i> , <i>Af</i>)) | (<i>Ly</i> (<i>Na</i> , <i>Li</i>)) |
|-------------------------------|--|--|--|
| RAxML (gene & codon position) | 37 | 35 | 27 |
| RAxML (gene) | 40 | 36 | 24 |
| MrBayes | 0.28 | 0.59 | 0.12 |
| BEAST | 0.88 | 0.08 | 0.04 |

Table 4. Comparisons of fit of data to three trees with alternative best-supported resolutions of the sister-group relationships of *Lycognathophis seychellensis* for the 21-leaf concatenated mt and nu data. Above the diagonal are SH and AU test p values, respectively, for differences between ML trees. See Table 3 for support for each phylogenetic resolution. Below the diagonal are Bayes Factor scores for path (and stepping stone) sampling results under Bayesian analysis. * indicates best-supported resolution under MrBayes analysis; ** best-supported resolution under BEAST analysis. See Table 3 for abbreviations of genera.

| | (<i>Ly</i> ((<i>Na</i> , <i>Li</i>)(<i>Hy</i> , <i>He</i> , <i>Af</i>))) | (<i>Ly</i> (<i>Na</i> , <i>Li</i>)) | (<i>Ly</i> (<i>Hy</i> , <i>He</i> , <i>Af</i>)) |
|--|---|--|--|
| (<i>Ly</i> ((<i>Na</i> , <i>Li</i>)(<i>Hy</i> , <i>He</i> , <i>Af</i>)))* | | 0.418; 0.298 | 0.501; 0.401 |
| (<i>Ly</i> (<i>Na</i> , <i>Li</i>)) | 1.2 (1.1) | | 0.772; 0.682 |
| (<i>Ly</i> (<i>Hy</i> , <i>He</i> , <i>Af</i>))** | 4.0 (3.9) | 2.8 (2.8) | |

Table 5. Estimates of age (in Ma) of divergence between *Lycognathophis seychellensis* and its closest living (mainland sub-Saharan African) relative, for trees consistent with the three best-supported resolutions of the sister group of *L. seychellensis*. Results reported for TreePL and BEAST2 analyses of 73-leaf dataset. Values are means, with 95% highest posterior density interval in square brackets; values in and not in parentheses are from analyses implementing GTR and HKY models of sequence evolution, respectively.

| Analysis | <i>L. seychellensis</i> sister group | | |
|----------|--|---|--|
| | (<i>Hy, He, Af</i>) | ((<i>Na, Li</i>)(<i>Hy, He, Af</i>)) | (<i>Na, Li</i>) |
| TreePL | 35.68 (38.57) | 39.31 (39.31) | 41.27 (41.53) |
| BEAST2 | 35.31 [24.57–43.19] (43.09 [28.14–47.06]) | 43.34 [27.83–47.18] (42.41[27.06–47.82]) | 29.35 [24.11–37.84] (29.42 [25.51–39.28]) |

Table 6. Comparison of four models of ancestral area estimations implemented using BioGeoBEARS. Abbreviations: Ln L, log-likelihood; *d*, dispersal; *e* extinction; *j* jump parameter; *k*, number of parameters. AIC scores (sc) and weights (wt) are reported.

| Model | Ln L | <i>K</i> | <i>d</i> | <i>e</i> | <i>j</i> | AIC sc | AIC_wt |
|--------------------|--------|----------|----------|----------|----------|--------|--------|
| DEC | -8.55 | 2 | 0.0000 | 0.0000 | 0.00 | 21.110 | 0.210 |
| DEC+ <i>j</i> | -7.08 | 3 | 0.0000 | 0.0000 | 0.05 | 20.170 | 0.330 |
| DIVALIKE | -11.14 | 2 | 0.0033 | 0.0029 | 0.00 | 26.280 | 0.016 |
| DIVALIKE+ <i>j</i> | -7.3 | 3 | 0.0000 | 0.0000 | 0.06 | 20.600 | 0.270 |

FIGURE CAPTIONS

Fig. 1. Global distribution of sub-Saharan African (including Seychelles) natricine genera based on data from GBIF, Nagy et al. (2014), Chippaux & Jackson (2019), Conradie et al. (2020) and specimen vouchers from Port Elizabeth Museum (PEM). These genera comprise 14 currently recognised extant species as follows: *Afronatrix* (1 species), *Helophis* (1), *Hydraethiops* (2), *Limnophis* (3), *Lycognathophis* (1), and *Natriciteres* (6). Occurrence data for the one Seychelles and six of the mainland sub-Saharan African natricine genera (all except *Helophis*) were downloaded from the GBIF database (GBIF, 2019). Distribution data for *Helophis* were taken from Nagy et al. (2014). Spatial data were mapped using ArcGIS v. 10.5. (ESRI, The Redlands, CA). Sampling localities in mainland sub-Saharan Africa are labelled with numbers corresponding to those in Table 1. Precise locality information for *L. seychellensis* is presented in Table 1.

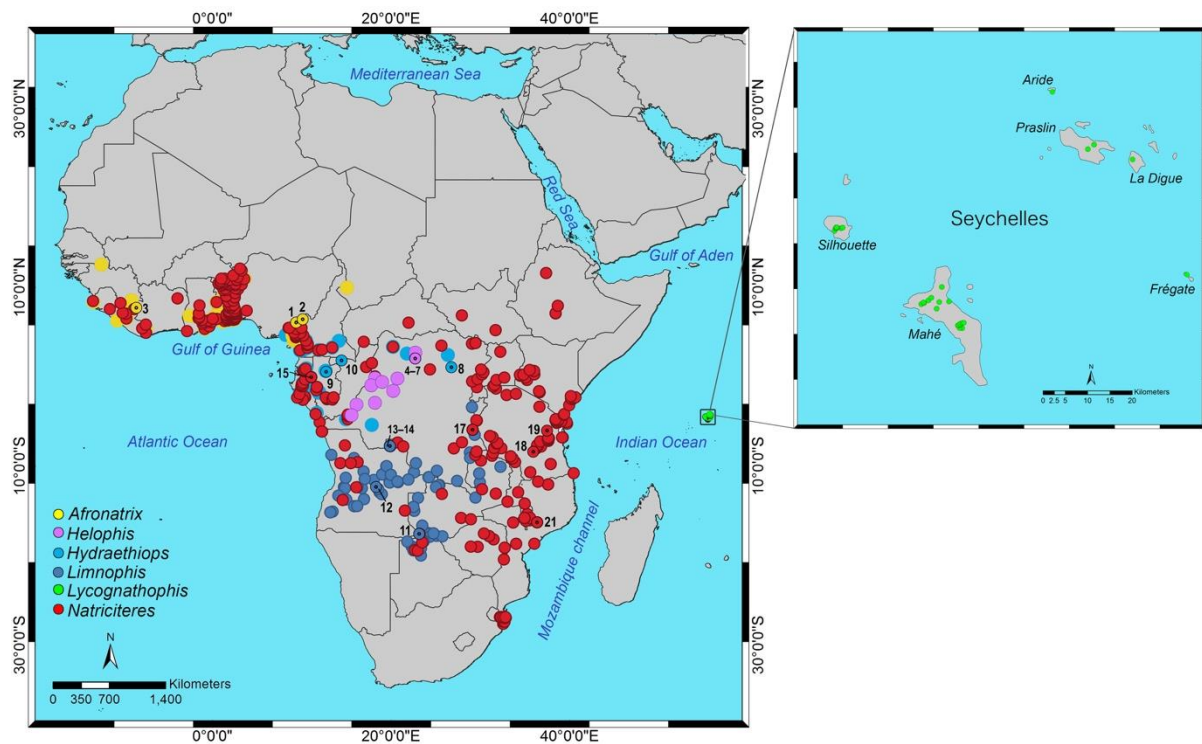


Fig. 3. BEAST chronogram showing divergence times for Seychelles and other (mainland) sub-Saharan African natricine snakes inferred from the 73-leaf, concatenated mt and nu dataset. Numbers at internal branches indicate mean divergence ages, with blue bars showing 95% highest posterior density intervals. Seychelles-Africa divergence is indicated with a *. Numbers in parentheses are sample codes (see Tables 1 and 2). See Fig. S2 for complete tree, including non-natricine alethinophidians, and values of 95% highest posterior density intervals. Ancestral area estimations (DEC + *j* model) at nodes represent areas before an inferred instantaneous speciation event, coloured boxes at tips indicate the current distribution of extant species.

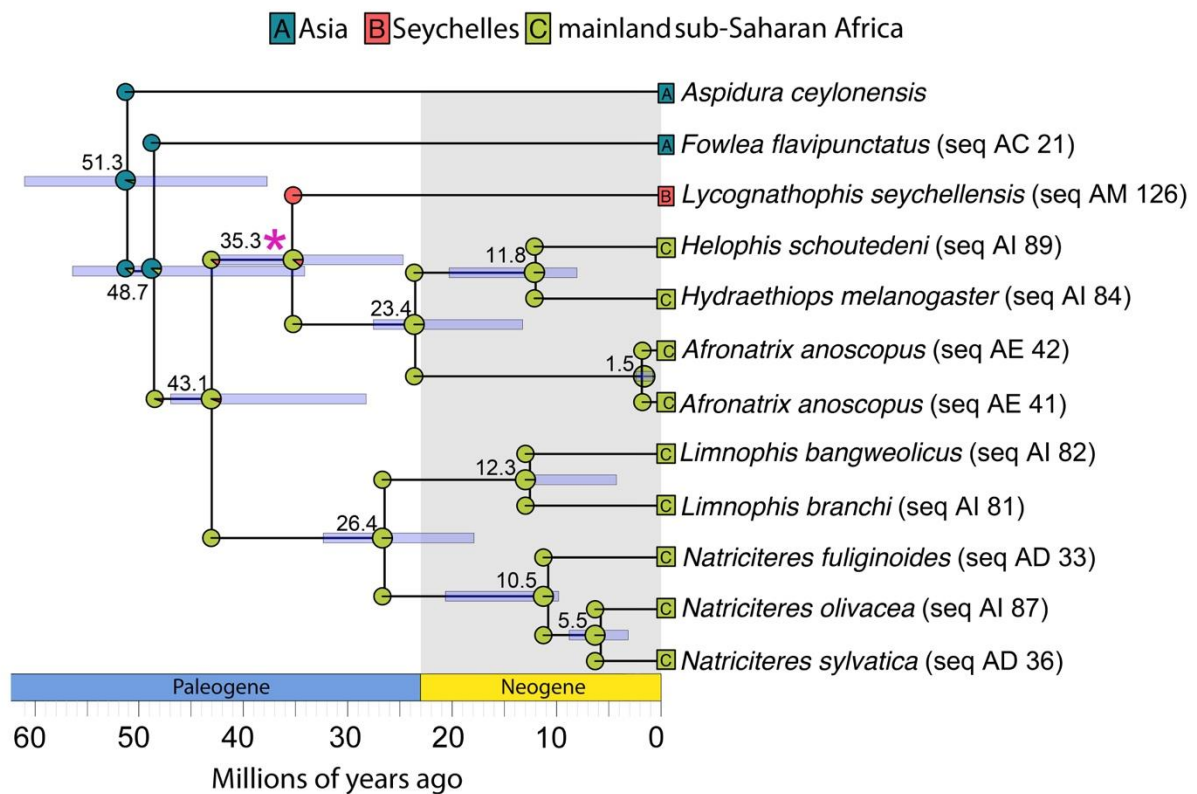
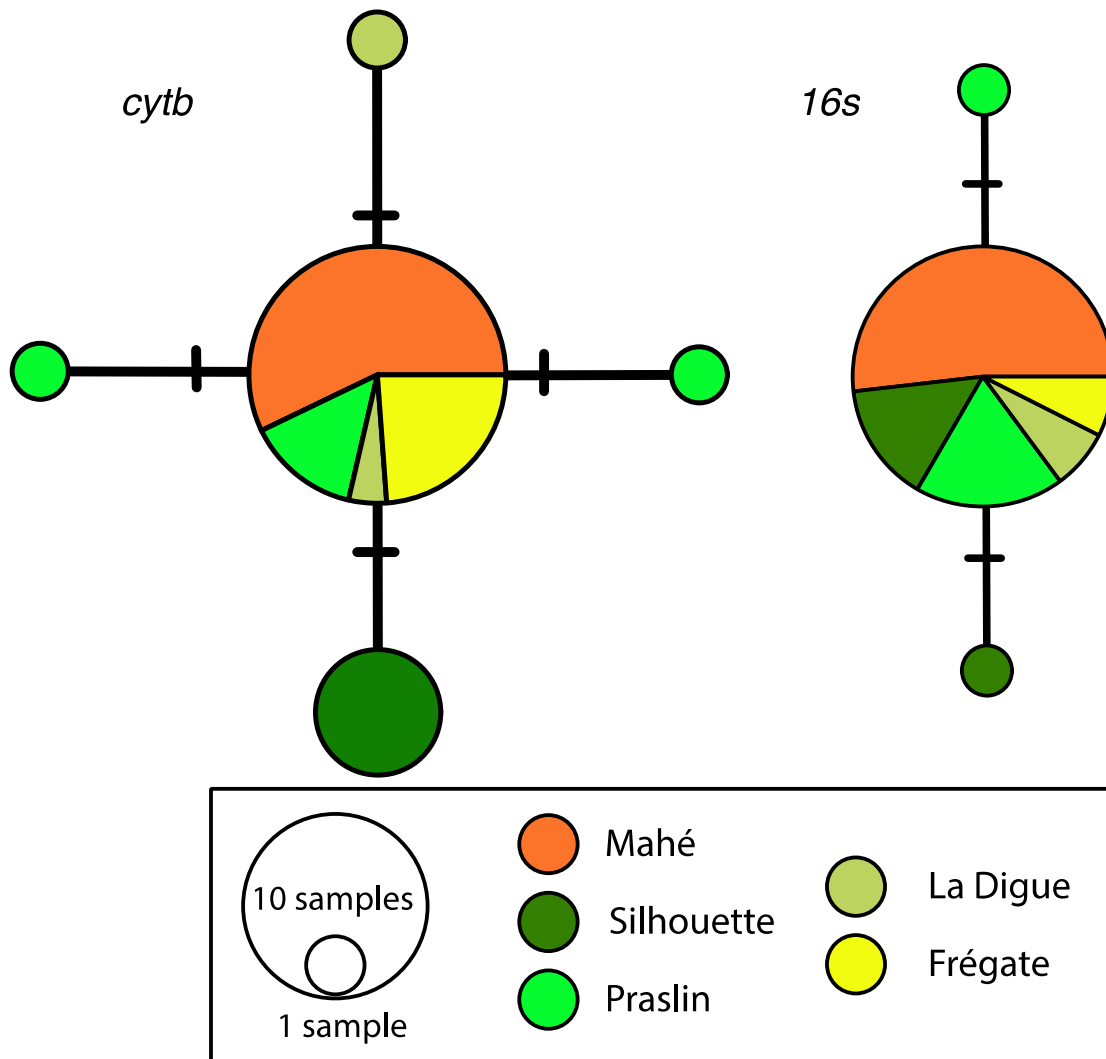


Fig. 4. Haplotype networks for mitochondrial *cytb* (n = 29) and *16s* (n = 30) for *Lycognathophis seychellensis* from five Seychelles islands using the median-joining (MJ) network algorithm. See Table 1 for sample and locality details.



Electronic supplementary material

Table S1. Primers used in this study for amplifying and sequencing target genes.

Table S2. Sequences used in the 157-leaf dataset, plus the two *Lycognathophis seychellensis* from GenBank (Vidal et al, 2008), which were used in this study only to calculate genetic distances. Sequences used in the 21-leaf dataset are indicated with *, outgroups are indicated with †, "-" = no data available

Table S3. Partitions and models of sequence evolution employed in analyses of the 73-leaf dataset. 1st, 2nd and 3rd denote codon position for protein-coding genes.

Table S4. Parameter values for fossil calibrations used in the BEAST divergence dating analysis. Ages in Ma. All maximum ages soft, except hard maximum for calibration 6.

Table S5. Partitions and models of sequence evolution employed in analyses of the 21-leaf dataset. 1st, 2nd and 3rd denote codon position for protein-coding genes.

Table S6. Support values for three incompatible clades representing the three competing resolutions of the relationships of *L. seychellensis* and other (mainland) sub-Saharan African natricines for the 21-leaf dataset. Values in each cell are given separately for analyses of mt - nu - mt+nu data (in that order). Highest support values for each analysis are highlighted in bold.

Fig. S1. A. Maximum Likelihood phylogeny and B. Bayesian phylogeny for the 157-leaf dataset.

Fig. S2. BEAST2 chronogram generated using concatenated-gene showing divergence times for natricine snakes and other alethnophidian snakes. Numbers at internal branches indicate posterior probabilities. Error bars indicate 95% highest posterior densities for node ages. Nodes C1–C7 are the seven calibrated nodes.

Fig. S3. BEAST2 chronogram generated using concatenated-gene with models of sequence evolution as suggested by partition finder. Numbers at internal branches indicate node ages. Error bars indicate 95% highest posterior densities for node ages.